2-2019

# DEVELOPMENT OF PIEZOELECTRIC SENSORS AND METHODOLOGY FOR NONINVASIVE SIMULTANEOUS DETECTION OF MULTIPLE VITAL SIGNS

Areen Abdallah Romi Allataifeh

United Arab Emirates University

College of Engineering

DEVELOPMENT OF PIEZOELECTRIC SENSORS AND
METHODOLOGY FOR NONINVASIVE SIMULTANEOUS
DETECTION OF MULTIPLE VITAL SIGNS

Areen Abdallah Romi Allataifeh

This dissertation is submitted in partial fulfilment of the requirements for the degree
of Doctor of Philosophy

Under the Supervision of Dr. Mahmoud Al Ahmad

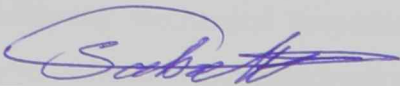February 2019

# Declaration of Original Work

I, Areen Abdallah Romi Allataifeh, the undersigned, a graduate student at the United Arab Emirates University (UAEU), and the author of this dissertation entitled *"Development of Piezoelectric Sensors and Methodology for Noninvasive Simultaneous Detection of Multiple Vital Signs"*, hereby, solemnly declare that this dissertation is my own original research work that has been done and prepared by me under the supervision of Dr. Mahmoud Al Ahmad, in the College of Engineering at UAEU. This work has not previously been presented or published, or formed the basis for the award of any academic degree, diploma or a similar title at this or any other university. Any materials borrowed from other sources (whether published or unpublished) and relied upon or included in my dissertation have been properly cited and acknowledged in accordance with appropriate academic conventions. I further declare that there is no potential conflict of interest with respect to the research, data collection, authorship, presentation and/or publication of this dissertation.

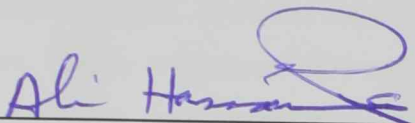Student's Signature: _____ Date: 30/4/2019

This Doctorate Dissertation is accepted by:

Dean of the College of Engineering: Prof. Sabah Alkass

Signature _____ Date _29/4/2019_

Acting Dean of the College of Graduate Studies: Prof. Ali Al-Marzouqi

Signature ___Ali Hassan___ Date ___23/5/2019___

Copy _1_ of _5_

# Approval of the Doctorate Dissertation

This Doctorate Dissertation is approved by the following Examining Committee Members:

1) Advisor (Committee Chair): Dr Mahmoud Al Ahmad

   Title: Associate Professor

   Department of Electrical Engineering

   College of Engineering

   Signature _____    Date _29.02.2019_

2) Member: Dr Mohammad Shakeel Laghari

   Title: Associate Professor

   Department of Electrical Engineering

   College of Engineering

   Signature _____    Date _28-02-2019_
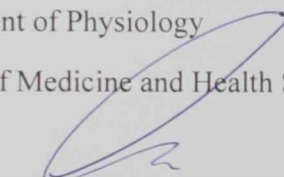
3) Member: Dr Frank Christopher Howarth

   Title: Professor

   Department of Physiology

   College of Medicine and Health Sciences

   Signature _____    Date _28/2/19_

4) Member (External Examiner): Dr. Michael Pecht

   Title: Professor

   Department of Applied Math, also Mechanical Engineering

   Institution: Maryland University, USA

   Signature _____    Date _21/2/19_

# Declaration of Original Work

I, Areen Abdallah Romi Allataifeh, the undersigned, a graduate student at the United Arab Emirates University (UAEU), and the author of this dissertation entitled "*Development of Piezoelectric Sensors and Methodology for Noninvasive Simultaneous Detection of Multiple Vital Signs*", hereby, solemnly declare that this dissertation is my own original research work that has been done and prepared by me under the supervision of Dr. Mahmoud Al Ahmad, in the College of Engineering at UAEU. This work has not previously been presented or published, or formed the basis for the award of any academic degree, diploma or a similar title at this or any other university. Any materials borrowed from other sources (whether published or unpublished) and relied upon or included in my dissertation have been properly cited and acknowledged in accordance with appropriate academic conventions. I further declare that there is no potential conflict of interest with respect to the research, data collection, authorship, presentation and/or publication of this dissertation.

Student's Signature: _____  Date: _____

# Advisory Committee

1) Advisor:  Mahmoud Al Ahmad

Title: Associate Professor

Department of Electrical Engineering

College of Engineering


2) Member: Ioannis Zuburtikudis

Title: Professor

Department of Chemical and Petroleum Engineering

College of Engineering

# Abstract

The activity of piezoelectric material linked the applied electric field with the strain generated that can be translated in to geometrical variations. Flexible steel substrate exhibits fascinating mechanical properties which enables their integration into the emerging field of flexible microelectronics. This work presents an extended technique based on capacitance-voltage dependency to extract the geometrical variations in thin film piezoelectric materials deposited on flexible steel. A 50 µm flexible steel sheet has been sandwiched by two PZT film layers, each of 2.4 µm in thickness deposited by sputtering. Aluminum layer of 370 nm has been deposited above each PZT layer to form the electrical contact. The steel sheet represents the common electrode for both PZT structures. Gamry references 3000 analyzer was used to collect the capacitance voltage measurements then estimating piezoelectric charge constant. Experimental work has been validated by implementing the same method on a bulk piezoelectric film. Results have showed that the measured capacitance varies by 1% due to dielectric constant voltage dependency. On the other hand, 99% of capacitance variations depend on the change in physical dimensions of the sample via piezoelectric effect. Further to that, this thesis explores the utilization of piezoelectric based sensors to collect a corresponding representative signal from the chest surface. The subject typically need to hold his or her breath to eliminate the respiration effect. This work further contributes to the extraction of the corresponding representative vital signs directly from the measured respiration signal. The contraction and expansion of the heart muscles, as well as the respiration activities, will induce a mechanical vibration across the chest wall. This vibration can be converted into an electrical output voltage via piezoelectric sensors. During breathing, the measured voltage signal is composed of the cardiac cycle activities modulated along with the respiratory cycle activity. The proposed technique employs the principles of piezoelectric and signal-processing methods to extract the corresponding signal of cardiac cycle activities from a breathing signal measured in real time. All the results were validated step by step by a conventional apparatus, with good agreement observed.

**Title and Abstract (in Arabic)**

# تطوير أجهزة الاستشعار الكهرضغطية والمنهجية للكشف المتزامن للعلامات الحيوية المتعددة

*الملخص*

المواد الكهرضغطية تربط الحقل الكهربائي التطبيقي بالتوتر المولد التذي يمكن ترجمته إلى اختلافات جيومترية. إن الركيزة الفولاذية المرنة تتميز بخصائص ميكانيكية رائعة تمكنها من الاندماج في المجال الناشئ للإلكترونيات الدقيقة المرنة. يقدم هذا العمل تقنية موسعة تعتمد على السعة والجهد لاستخراج التغيرات الجيومتريه الهندسية في المواد الكهرضغطية للفيلم الرقيق المودعة في الفولاذ المرن. تم وضع صفائح فولاذية مرنة بقطر 50 ميكرومتر بواسطة طبقتين من طبقات الفيلم PZT ، كل منها يبلغ سمكه 2.4 ميكرومتر يتم ترسيبه بواسطة الرش. طبقة الألومنيوم من 370 نانومتر ترسبت فوق كل طبقة PZT لتشكيل الاتصال الكهربائي. تمثل ورقة الصلب القطب المشترك لهياكل PZT. تم استخدام جهاز Gamry 3000 محلل لجمع قياسات الجهد و السعة ثم تقدير ثابت الكهرضغطية. تم التحقق من صحة العمل التجريبي من خلال تطبيق نفس الطريقة على فيلم كهرضغطية كبير. أظهرت النتائج أن السعة المقاسة تختلف بنسبة 1٪ بسبب تبعية الجهد الثابت للكهرباء. من ناحية أخرى ، تعتمد نسبة 99٪ من تغيرات السعة على التغيير في الأبعاد المادية للعينة تحت تأثير الكهرضغطية. علاوة على ذلك ، تستكشف هذه الأطروحة استخدام أجهزة الاستشعار الكهرضغطية القائمة لجمع إشارة تمثيلية مقابلة من سطح الصدر. يحتاج الشخص عادةً إلى ضبط نفسه لالغاء تأثير التنفس. ويساهم هذا العمل أيضًا في استخراج العلامات الحيوية التمثيلية المقابلة مباشرةً من إشارة التنفس المقاسة. إن تقلص عضلات القلب وتوسعها ، بالإضافة إلى أنشطة التنفس ، ستحفز الاهتزاز الميكانيكي عبر جدار الصدر. يمكن تحويل هذا الاهتزاز إلى جهد خرج كهربائي عبر أجهزة استشعار كهرضغطية. أثناء التنفس ، تتكون إشارة الجهد المقاسة من نبض القلب المشكّلة جنبًا إلى جنب مع نشاط التنفس. تستخدم التقنية المقترحة مبادئ طرق كهرضغطية وطرق معالجة الإشارات لاستخراج الإشارة المقابلة لأنشطة القلب من إشارة التنفس المقاسة في الوقت الحقيقي. تم التحقق من صحة جميع النتائج خطوة بخطوة من قبل جهاز تقليدي، مع ملاحظة تطابق جيد في النتائج.

**مفاهيم البحث الرئيسية**: اعتماد مكثف على السعة، تنفس، ثابت كهرضغطية، جهد ثابت، دورة تنفس، دورة قلبية، شحنة ثابتة، ضغط الدم، مستشعرات كهرضغطية، مستشعرات مرنة، معالجة إشارة، غشاء رقيق ، نبضات.

# Acknowledgements

Foremost, I would like to extend my appreciation to my advisor, Dr. Mahmoud Al Ahmad. He gave me a precious opportunity to work with him and motivated me throughout the work. I'm thankful for being my tutor and for his wise aspiring guidance.

I also would like to thank Professor Manos Tentzeris for the opportunity he gave me working in his laboratory at the Georgia Tech University for three months. I express my fully gratefulness to my parents for their guidance and support.

I will never forget to thank my dear friends for being there for me supporting and encouraging me all time.

# Dedication

*To my beloved parents and family*

# Table of Contents

# List of Tables

# List of Figures

# List of Abbreviations

| | |
|---|---|
| AlN | Aluminum nitride |
| BAW | Bulk acoustic wave |
| BCG | Ballistocardiogram |
| BP | Blood pressure |
| CV | Capacitance-voltage |
| DP | Diastolic pressure |
| ECGs | Electrocardiograms |
| EDV | End-diastolic volume |
| EIT | Electrical impedance tomography |
| ICA | Independent component analysis |
| LDV | Laser doppler voltmeter |
| MEMS | Micromechanical systems |
| PCA | Principle of component analysis |
| PFM | Piezoelectric electron force microscopy |
| PPG | Photoplethysmography |
| PVDF | Polyvinylidene flouride |
| PZT | Lead zirconate titanate |
| RF | Radio frequency |
| RR | Respiration rate |
| SFCW | Stepped frequency continuous wave |
| SP | Systolic pressure |
| XRD | X-ray diffraction |
| ZnO | Zinc dioxide |

# Chapter 1: Introduction

## 1.1 Motivation

Cardiac cycle monitoring plays an important role in providing essential information for daily health monitoring and medical diagnosis [1]. Lately, cardiac cycle monitor based systems development has attracted the attention [2-4]. The basic concept after this development incorporates capturing and analyzing various cardiac signals and extract several corresponding features and parameters [5]. The extracted features will enable effective safeguarding of cardiac health by allowing early diagnosis of any diseases or abnormalities [6-8].

Both heart and lungs physiological cycle activities induce mechanical vibrations inside the chest wall [9]. These vibrations are highly correlated with the respiration rate and cardiac cycle features [10]. When a piezoelectric sensor is placed on the exterior surface of the chest, such induced vibrations will act as a mechanical load on the piezoelectric sensor. The piezoelectric sensor correspondingly produces an electrical voltage signal that is conformally mapped with both respiration and cardiac activity [11]. The structure of the piezoelectric sensor plays an essential role in enhancing the output voltage representative signal due to respiration as well as heart beats [12]. Therefore; different structures have been developed and studied during the last decade to enhance this performance. Cantilever structures are the most used types [13, 14]. Other utilized structures are ring shape [15], cylinder [16], and sandwich [17].

Commercially, lead zirconate titanate (PZT) is a common piezoelectric material that is used for piezoelectric sensors and actuators due to its high piezoelectric

voltage constants [18, 19]. On the other hand, PZT is considered to be a ceramic material which limits its ability to adapt to curved surfaces [20]. This also in turn affect the sensitivity of the sensor or actuator devices [21]. To overcome such issues, several PZT materials were deposited on flexible substrates using various technologies [22-24]. As a consequence, several flexible piezoelectric sensors have been introduced in biomedical applications due to their highly piezoelectric, lightweight, slim, and biocompatible properties [25, 26]. Batteries and wires are another issue in cardiac monitoring devices. Furthermore, rare attempts have been carried out to utilize a double-face PZT flexible structures for the development of self-powered monitoring systems [27].

The acquired output voltage signal of the piezoelectric placed atop a human chest is most likely to be composed of heartbeat, respiration activities and other noises such as human movements [28]. Many researchers have developed techniques and methods to eliminate the noise effect and remove the respiration activities contributions [29]. Nevertheless, there is still a need to develop a robust system and methodology that is able to noninvasively extract simultaneous multiple vital signs using innovative approaches.

## 1.2 Literature Overview

Monitoring vital signs is essential for health and medical diagnosis [30]. Vital signs such as ECG, heartbeat [31], respiration rate [32], and systolic and diastolic blood pressures [33] along with pressure pulse play an important role in determining the state of health of a subject [34]. Various methods and systems have been developed to monitor such vital signs [35-40]. These vital signs are extracted from the acquired

signals that enable more effective safeguarding of health by allowing early detection of any diseases or abnormalities [41-43]. Researchers have been focusing on developing remote non-contact sensing systems having the ability to perform long-term, accurate, and continuous monitoring of human vital signs. Measuring vital signs (such as respiration rates, blood pressure, and heart rates) continuously and remotely without touching the patients can be a priceless tool for physicians. Better and more rapid life-and-death decisions when the long-term patient data are available [44]. Monitoring vital signs systems will prevent diseases and enhance quality of life, thus reducing costs of health care costs [45].

### 1.2.1 Piezoelectric Materials Constants Extraction

Piezoelectric materials special characteristics that enable them to control flexible structures and sensing fields [46]. Such materials have been integrated and incorporated within highly adaptive smart structures [47]. Flexible piezoelectric thin films have been implemented in biomedical applications due to their highly piezoelectric, lightweight, slim, and biocompatible properties [48, 49]. Commercially, PZT is a common piezoelectric material that is used for piezoelectric sensors and actuators [50, 51]. On the other hand, the monolithic PZT piezoelectric wavers or patches, including ceramic materials, have poor fatigue resistance and are very fragile [52]. That limits their ability to adapt to curved surfaces and makes them vulnerable to breakage accidently through bonding and handling procedures [53]. This in turn affects the sensitivity of the sensor or actuator devices [54]. To overcome these issues, PZT deposited on flexible sheets [55].

The piezoelectric thin films on flexible sheets respond to nanoscale biomechanical vibrations caused by acoustic waves and tiny movements on corrugated

surfaces of internal organs [56]. Furthermore, it is used for developing self-powered energy harvesters, as well as sensitive nano-sensors for diagnostic systems [57]. Flexible sheets of PZT material are naturally tough and pliable unlike the traditional piezoelectric patches [58]. Xu et al. have developed a piezoelectric tape that is composed of patterned packed PZT elements sandwiched between two flexible metallic films. The PZT elements can have various distribution densities and shapes. This phased array piezoelectric tape has good conformability to curved surfaces which makes it suitable to be used in different mechanical structures [59].

An apparent knowledge of material characteristics, including the piezoelectric coefficients and the electromechanical coupling factors, is necessary for using the piezoelectric thin films in micromechanical systems (MMES). Uskoković et al. compared the resulting piezoelectric coefficient values with other materials [60]. Jackson et al. compared between capacitance-voltage (CV) method [61], laser Doppler vibrometer (LDV) [62], Berlincourt [63], and piezoelectric force microscopy (PFM) method [64] to find piezoelectric properties of aluminum nitride (AlN). They concluded that LDV and PFM are the most accurate methods, but the CV method is the easiest and quickest method to use [65]. Hemert et al. elaborated on the CV measurements and proposed a bias independent capacitance model as an alternative. They extracted from their proposed model $d_{33}$ and k, then verified the results at various biased electrode thicknesses. They have used a bulk acoustic wave (BAW) resonator model as a bias dependent capacitance model for piezoelectric capacitors. Using this model, the piezoelectric coefficient $d_{33}$ and dielectric constant were extracted from CV recordings for three different layer thicknesses [66].

On the other hand, Hemert et al. criticized the CV method in other research as

they concluded that the permittivity is not constant, so the piezoelectric parameters need further information to be determined by the CV measurement such as the resonance measurements [67]. Zhang et al. took AlN properties and studied the coefficients of AlN films by microscopy measurement and finite element method; they criticized the capacitance method due to the effect of interfacial capacitance between PZT films and electrodes as well as its low precision [68].

**1.2.2 Piezoelectric Extraction of Cardiac and Respiratory Parameters**

Vital signs such as ECG, heartbeat [69], respiration rate [70], systolic, and diastolic blood pressures [71] along with pressure pulse play an important role in determining the state of health of a subject [72]. Monitoring vital signs is essential for daily health and medical diagnosis [73]. Various methods and systems have been developed lately to monitor such vital signs [74-80]. These vital signs are extracted from the acquired signals that enable more effective safeguarding of health by allowing early detection of any diseases or abnormalities [81-83]. Researchers have been focusing lately on developing a remote non-contact sensing systems having the ability to perform long term, accurate, and continuous monitoring of human vital signs. Measuring vital signs (such as respiration rates, blood pressure, and heart rates) continuously and remotely without touching the patients can be a priceless tool for physicians, which is utilized for making life-and-death decisions rapidly and making better decisions when the long-term patient data are available [84]. Monitoring vital signs systems will prevent diseases and enhance quality of life; thus, reduce decrease costs of health care [85]. Furthermore, portable monitors improves our understanding of sleep pathophysiology and physiology which is significance goal for medical wellness reasons and assessing sleep at home without the need of hospitalizing.

Repeated measurements, self-experimentation, and evaluation of temporal patterns are achieved by portable monitors. That will allow individualized treatment decisions, improve disease phenotyping, and individualized health optimization. From here comes the need for developing continuous vital signs monitors [86].

Noninvasive vital sign monitoring, which includes measurement of pulse oximetry [87], capnography, blood pressure (BP) measurement, and the standard five-lead electrocardiogram [88], has been used for patients who are in the intensive care unit [89] and in the operating room. A stepped frequency continuous wave (SFCW) radar is also used to measure the heart rate and respiration by transmitting high average power pulses with long duration and narrow bandwidth; then, a signal-processing algorithm based on the state space method is applied to extract cardiac and respiration rates from the data measured on a human subject using SFCW radar [90]. Other noninvasive sensors have been implemented in the field, for example, photo-plethysmography (PPG) sensors, which operate by observing the effect of blood engorgement and composition on light absorption during the systole phase [91]; Furthermore, ECG devices that have a capacitive electrode with a shield over conductive foam; and household monitors for heart rate based on ECG techniques using a chest strap [92].

The main methodology used for cardiac health analysis involves capturing and analyzing the various cardiac signals and parameters [93, 94]. Various methods and devices have been lately developed to monitor cardiac cycle such as photoplethysmography (PPG) sensor which operates by observing the effect of blood engorgement and composition on light absorption during systole phase [95], electrocardiograms (ECGs) devices that has a capacitive electrodes with a shield over

a conductive foam; household monitors for heart rate based on ECG techniques on chest strap are commercialized, but they are not inconvenient for long-term usage [96],Shin et al. have used the ballistocardiogram (BCG) signal to estimate heart rate variability and analyze the cardiac autonomic modulation [97]. Kortelainen and Pärkkä recorded ballistocardiographic (BCG) data for subjects during normal sleep, and managed to extract heart rate and respiration signal using multichannel algorithms. They used Fourier Transform to extracted heart rate and calculated the respiration signal [98]. Another researchers used ECG, BCG and PPG to determine blood pressure and heart rate variability. They reported that ECG and PPG are more accurate than BCG, due to the fact that ECG has sharp complex event labeled with QRS, Furthermore, the regularity of PPG signal allows good detection of events. On the other hand, the diminished characteristics of the BCG make it more complicated signal to process [99].

Many researchers have developed techniques to capture the cardiac cycle corresponding signals and separate it from noises as well from other important vital signs such as respiration. Rahman et al. have implemented an independent component analysis (ICA) in the electrical impedance tomography (EIT) to separate the cardiac and respiration signals from each other. Experiments were implemented using a 16 channel EIT device, the electrodes of the channels were placed around the thorax circumferentially. It was performed for only 40s and not designed for continuous monitoring, and even if it could be enhanced, the hardware of makes it uncomfortable for long time use    [100]. Deibele et al. have utilized the principle of component analysis (PCA), which is a statistical method, to identify time domain filtering in separating the two vital signs. They used two types of filters; FIR to suppress noise of higher frequency as well as ventilation lower frequency. the results doesn't reveal the

ECG real shape due to the low sampling rate that make it more sensitive to noises. Furthermore, there is a major drawback for using this method is that the EIT images changes due to changes in blood vessels volume, but volume variations in greater vessels doesn't certainly specify blood flow on capillaries [101]. Using wearable devices in monitoring heart failure remotely reduces hospitalizations and allows to assess heart failure states as well as tracking clinical status in the future for outpatients with heart failure [102].

In the same context, the respiration cycle lengths were determined from electrocardiographic (ECG) signal for detection sleeping disorders and estimating sleeping quality. Vehkaoja et al. extracted R-peaks and respiratory sinus arrhythmia from ECG signal at breathing recorded using textile electrodes tied to bed sheets, they did not completely separated the two vital signal, nevertheless, they extracted the respiration parameters while sleeping with the help ECG signal [103]. Bifulco et al. have extracted the cardiac cycle by simply filtering the piezoelectric signal [104]. Others have generated piezoelectric signal form chest that was separated into respiration, motion, and ballistocardiogram (BCG) waveforms by the use of proprietary algorithm, the method was not robust enough in extracting the respiration rate due to difficulty for finding RR reference value [105].

Piezoelectric transducers have been used as well to monitor cardiac cycle, they could be divided into two main groups; single element piezoelectric transducer or multiple elements transducers [106]. Each element in the array of transducers could be shaped as concave [107], convex [108], or plane elements [109]. Piezoelectric pressure sensors have been used in sleep monitoring to detect sleep related breathing disorders. They used eight piezoelectric sensors to detect movements and fund that it

is a promising method to be used at home monitoring [110]. Another researchers have planted piezoelectric sensors under the mattress to analyze sleep and collect vital signs. They compared their results with PSG data and reported that the system shows a good sleep staging and collects respiratory and heart rate information with better performance compared with accelerometer-based systems [111]. Sato et al. proposed in his research a PZT cardiorespiratory monitor system which is composed of disk-shaped PZT sensor, two band-pass filters, a breathing movement detector, a cardiac beat detector, microprocessors and a temperature controller. The PZT sensor is mounted in a plate made of copper covered by insulating sheets with thickness of 0.5 mm and all placed on an electronic controlled heater. The system collects electrical signal of heart beats and manages to separate it from the respiration noise [112]. The drawbacks of this system that it contains many devices connected together, the wiring is an issue here.

Bifulco et al. extracted vital signs by simply filtering the piezoelectric signal. The patient's ECG signal was simultaneously recorded to provide a time reference of the cardiac activity. The piezoelectric sensor was able to record respiratory movements, cardiac timing, and heart sounds. These signals can be obtained from the recorded signal by applying simple filters [113]. Klap et al. used a piezoelectric sensor to measure respiration and extract ballisto-cardiogram (BCG) waveforms using a proprietary algorithm. The method was not sufficiently robust in extracting the respiration rate because of the difficulty of finding the respiration rate (RR) reference value due to environmental noise [114].

Mizuno and Manhtliep developed a signal-processing algorithm to extract the essential vital signs from a noisy signal. They focused on monitoring the heart rate of

drivers to determine the drowsiness level for safe driving. They adopted seat-embedded piezoelectric sensors to detect the heart rate of the driver. These sensors measure the body vibration caused by the heartbeat, but the signal also contains a large amount of car body vibrations based on the road conditions. To overcome this issue, Mizuno et al. proposed a heart rate detection system based on the on-line adaptive filtering technique. The proposed system has a simple structure compared with the offline time-series model (ARX model)-based system and similar performance [115].

Al Ahmad et al. proposed the use of a piezoelectric sheet as a contactless cardiac cycle sensor to extract heart rate and blood pressure from the measured output voltage. The employed piezoelectric sheet captures the heart mechanical activities [116]. The generated electrical voltage is conformally mapped with the heart mechanical activity, as has been presented in another study [117]. The piezoelectric sensors were used in a bed-leaving detection system to monitor the vital signs of the body, such as the respiration rate, blood pressure and human body movements. Piezoelectric sensors were installed inside a pillow and under a mattress or futon. The signal differences between sleeping, awakening, and bed-leaving states were analyzed, leading to the development of a status classification method [118].

Al Taradeh et al. proposed a noninvasive piezoelectric-based method to count the heart rate [119]. The piezoelectric sheet was placed on the chest. The mechanical activity of the heart caused the sheet to deform, which produced a voltage signal. A mechanical model was developed based on the corresponding electrical waveform. The main constraint was that the signals were collected while the patient held his or her breath; thus, the method must be improved to eliminate the respiration constraint.

From the literature, it can be noticed that the previous work has many drawbacks, such as, complexity in data processing, wiring issues, or that it needs more than one sensor to extract the data. And none of the previous work has extracted a whole heart beat signal along with other vital signs at once. Furthermore, the blood pressure and heart beat rate were collected either by holding breath or by eliminating the breathing noises by another devices. In our work, single piezoelectric sheet is proposed with developed algorithm to extract multi vital signs at once and with the ability of extracting heart beat signal from respiration signal directly.

Using wearable devices in monitoring heart failure remotely reduces hospitalizations and allows to assess heart failure states as well as tracking clinical status in the future for outpatients with heart failure. The developed sensor allows for monitoring remotely respiration rate, heart rate, systolic and diastolic pressure, which allows to detect abnormalities early.

To efficiently monitor the patients, there is a need to let the monitoring continuously. The proposed device continually sends the data of the patient to their doctor in the hospital, which allows continuous checking on their health and detect any abnormalities early.

Portable monitors improves our understanding of sleep pathophysiology and physiology which is significance goal for medical wellness reasons and assessing sleep at home without the need of hospitalizing. Repeated measurements, self-experimentation, and evaluation of temporal patterns are achieved by portable monitors. That will allow individualized treatment decisions, and individualized health optimization. From here comes the need for developing our portable monitor.

Our proposed monitoring technique composed of only single piezoelectric sensor placed on the chest that sends the data by Bluetooth to a PC for processing. This single sensor collects the data of respiration and heart beats at once, then a developed algorithm extract multi vital signs such as respiration rate, heart rate, systolic and diastolic pressure.

The main advantage of this technique over the previous methods that it collects multi vital signs using a single piezoelectric sensor with small dimensions, which assures the comforts for the patients. The developed sensor is flexible which makes it more sensitive to small vibrations collected from the heart and reads the signals more accurate than bulk sensors.

Another advantage of the developed sensor that it could be placed anywhere on the abdomen even on the right side away from the heart and still have correct and accurate values. This criteria allows patients with special condition to monitor their heart condition; patients with heart failure use a pacemaker on the heart, it is difficult to monitor them continuously with electrical devices above the heart, so they can use this device on the left side of the abdomen. Other researchers collected vital signs from the ears, neck or fingers; the area of the abdomen permits to detect multi-vital signs related to heart and lungs.

The simplicity of the developed algorithm gives it more advantage over the work in the literature since it does not use filters or complex calculations. Furthermore, other researchers used the oscillators to eliminate the effect of noises, in our work we used the averaging method of the cycles to eliminate the effect of noises mathematically without the need of addition devices. That makes it more compact and less complex.

The inconvenience of placing too many sensors for monitoring bothers he patients. From this fact, the proposed monitoring technique only uses one device for sensing. That decreases the wiring used and let the patient to be comfortable for long time use.

In the previous work, some of the researchers used PVDF sensors in fabricating pressure sensors for vital signs monitoring. Our developed sensor was fabricated from PZT material, which has higher piezoelectric coefficients compared to the PVDF. The higher the piezoelectric coefficients, the more it become sensitive to vibrations. That makes our sensor more accurate and much efficient.

The flexible sheet has two PZT sides with stainless steel sheet sandwiched between them. The objective of fabricating two flexible sheets is to be able to collect two electric signal out from the vibration of the thorax. The idea here is to extract the vital sins from the first layer and be able to use the electric signal from the second layer for harvesting energy. That allow the sensor to be enhanced in the future to be self-powered sensor.

## 1.3 Research Objectives

This thesis explores the development and characteristics of a double-face piezoelectric sensor at the interface of PZT materials and flexible steel sheet. This work takes a close look at the use of capacitance-voltage measurements for the extraction of double piezoelectric thin film material deposited on the two faces of a flexible steel sheet.

The use of piezoelectric sensors to collect a corresponding representative signal from the chest surface requires the human subject to hold his or her breath in order to eliminate the respiration effect. This work further contributes to the extraction of the corresponding representative vital signs directly from the measured respiration signal.

This developed algorithm should allow to the heartbeat signal to be extracted from a respiration signal taken from the right side of the subject's chest. This is useful for situations in which electric cannot be near a patient's heart.

## 1.4 Research Significance

In the United Arab Emirates (UAE), common diseases, such as diabetes, obesity, and cardiovascular diseases, are observed according to UAE health research reported by Ministry of Health in 2016 [120]. Hence, the early diagnosis of diseases is a well-known critical step in disease treatment, prevention, and management and can even lead to a cure of the disease.

Heart patients usually need to stay in the hospital for continuous monitoring, however, portable monitors are available to carry on their normal activities while monitoring their health. These devices should be comfortable to wear and equipped with the fewest possible wires so the patient does not need to change batteries often.

A new algorithm proposed for extracting a heartbeat signal from the generated piezoelectric voltage signal that facilitate the development of new sensor generation to detect and identify any respiration, and heart abnormalities. This algorithm will have the ability to extract heart beat signals utilizing piezoelectric sensors placed away from the heart position, which makes it beneficial for patients with special conditions.

Compared with the work mentioned in [138] and [139], the proposed work represents a paradigm shift technique. The piezoelectric sheet sensor will provide non-invasive and contactless connections to capture both temporal respiration and holding breath signals from different locations of the subject's chest. Hence, there is no further need for holding breath to collect heart beats; the proposed procedure utilizes the effect of the inspiratory cycle.

The proposed sensor has two piezoelectric layers, one of them to collect the signal and the second one could be used to harvest energy and be self-developed sensor. Furthermore, The developed algorithm opens the opportunity to extract the ECG signal using the same developed algorithm.

The proposed technique is simple, reliable, and easy to handle, and causes minimal inconvenience to the patient as well as to clinics. The developed sensor is flexible and light weight, and is able to extract multiple vital signs at the same time solving many issues facing the patients nowadays.

## 1.5 Research Limitations

One of the limitations of the algorithm is that the piezoelectric sheet should be placed on the chest and abdomen area. It can not be positioned on any other place on the body because it depends on the respiration signal in the first place. Furthermore, the algorithm can handle small noises, such as speaking, eating, and small movements, while measuring; these noises can be removed from the averaging process. The algorithm must be further improved to counteract the effect of major noises that could occur while the subject is moving.

**1.6 Dissertation Organization**

This dissertation is organized as follows:

Chapter 1 (Introduction): This chapter introduces the main objective along with the significance and motivation. Furthermore, it reviews briefly the previous research related to this topic.

Chapter 2 (Fundamentals of piezoelectricity): This chapter summarizes the fundamental theorem of the piezoelectric effect and discusses the various techniques used to characterize piezoelectric materials.

Chapter 3 (Extraction of piezoelectric constants): This chapter develope a novel methodology to extract the piezoelectric constants of thin film materials using the capacitance voltage approach. It also analyzes and validates the results.

Chapter 4 (Noninvasive piezoelectric detection): This chapter discusses the proposed algorithm of extraction of the corresponding representative vital signs directly from the measured respiration signal. It reports the results gained from performing the experiments, describes the processing and analysis of data, and discusses the results and validation using a different technique.

Chapter 5 (Conclusions and Future Work): This chapter summarizes the research findings and relates them to the objectives presented in the first chapter and future work that could be performed to enhance and elaborate the work.

# Chapter 2: Fundamentals of Piezoelectricity

The functionality of piezoelectric materials is being exploited in many integrated applications due to their electrical-mechanical reciprocity [121-129]. Some types of piezoelectric materials require a polling process to activate their functionality [130]. This process can only be carried out at temperatures below the Curie point, when the crystal structures cause an electric dipole to be created. Indeed, the piezoelectric materials polar domains are distributed randomly before the polling process as depicted in Figure 1(a). In perovskite structures the dipole is created by movement of the central ion in the structure. The process of polling involves aligning all of these individual dipole moments, so that they all point in the same general direction as depicted in Figure 1(b). This is accomplished by putting the crystal in a constant electric field to force the dipoles to align. When the electric field is removed, the dipoles remain fairly aligned, although there will still be some element of random direction [131].

The most commonly used are PZT [132], zinc oxide (ZnO) [133], aluminum nitride (AlN) [134] and polyvinylidene difluoride (PVDF) [135]. Different methods have been used to measure the piezoelectric coefficients [62-67]. For these methods, the determination of the variation in physical dimensions, longitudinal and transversal, is the key for measuring the piezoelectric material parameters. For bulk ceramic materials, the most commonly used method to characterize the piezoelectric coefficients is based on using a dynamically varying load, i.e., Berlincourt technique, which offers a rapid and cost-effective method of assessing the piezoelectric constants [136]. The Berlincourt method is based on the direct measurements of force-induced charge. The calibration of the Berlincourt meter is usually carried out using the

provided standards. The resonance technique has also been used to measure the piezoelectric constants and assumes that samples are infinitely thin or infinitely long, and the corrections for finite dimensions must be considered [137]. A comparison between various piezoelectric materials is summarized in Table 1.
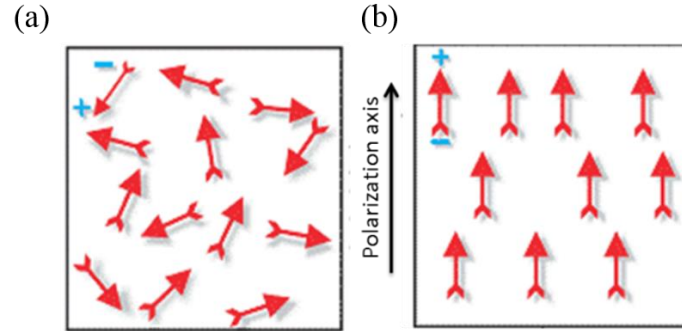


Figure 1: Piezoelectric materials polar domains orientations (a) before and (b) after polling process, after [131].

Recently a promising method of measuring the vertical extension of a piezoelectric thin film using an impedance analyzer was presented in [138, 139].

The proposed method uses the change in capacitance-voltage relation to characterize the physical properties. This type of characterization is an attractive alternative for several reasons. First, a standard LCR meter is used to get the measurement. Second, the technique does not require any kind of mechanical probe to measure the displacement, thus it is a non-invasive and destructive technique.

Table 1: Characteristics of various kinds of piezoelectric materials

| Property | PZT | ZnO | AlN | PVDF |
|---|---|---|---|---|
| $d_{33}$ | High | Moderate | Low | Low |
| $d_{31}$ | High | Moderate | Low | Low |
| Resistance | High | High | High | Low |
| constant | Huge | High | Low | Low |
| Sound velocity | High | Moderate | Low | Low |
| TEC | High | High | Low | Low |
| Ferroelectricity | Yes | Yes | No | Yes |
| Density | High | Low | Low | Low |
| CMOS | Not | Not fully | fully | NA |

## 2.1 Piezoelectric Theory

Piezoelectric materials generate a voltage signal proportional to applied stress [140]. Piezoelectric materials based sensors are used because they produce an output voltage is conformally map with the he acting mechanical stress. As has been demonstrated earlier by Al Ahmad and Al Shareef, when a piezoelectric sensor is placed atop the chest surface, it can detects the contraction and expansion of the heart muscle and produce a corresponding voltage [138].
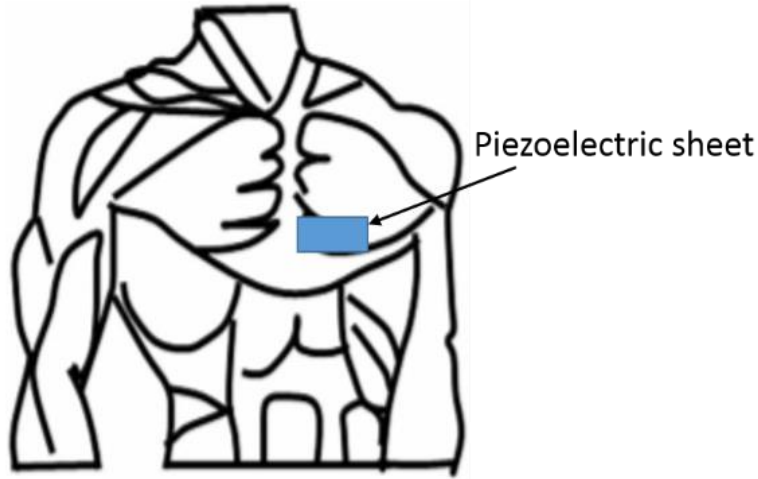
Figure 2: Placement of a piezoelectric sheet on the chest

Figure 2 illustrates a piezoelectric sheet placed on a human chest. The relation between the induced vibration in the chest and the corresponding output voltage can be represented as follows [141]:

$$P(t) = -nV(t) \tag{1}$$

Where $P(t)$ is the pressure resulting from the induced vibrations, $V(t)$ is the generated output voltage, and $n$ is the equivalent turns ratio of the piezoelectric sheet. The equivalent turn ratio can be calculated by the following formula [142]:

$$n = d_{33}c_p/t \tag{2}$$

Where $d_{33}$ is the piezoelectric charge constant, $c_p$ is the piezoelectric material elastic constant, and $t$ is the piezoelectric sheet thickness. The variation in output voltage ($\dot{V}$) and variation in applied stress ($\dot{V}$) is expressed as [143]:

$$\dot{V} = \frac{c_p t_c d_{31}}{\varepsilon} \dot{S} \tag{3}$$

where $\varepsilon$, $c_p$, $t_c$ and $d_{31}$ are the material dielectric constant, elasticity coefficient, thickness and piezoelectric voltage constant, respectively.

## 2.2 Capacitive-Voltage Approach

When a piezoelectric material is sandwiched between two electrodes subjected to either mechanical or electrical strains, its geometrical dimensions and dielectric constant will change according to the direction and magnitude of the applied field. Figure 3(a) illustrates a circular disk of a piezoelectric material without applying any type of field. When this disk is driven by applied electrical field with the direction opposite to the polling direction, the thickness decreases and the area increases simultaneously as depicted in Figure 3(b), resulting in an increase in capacitance. On the other hand, if the applied electric field is aligned with the polling direction, the thickness increases and the area decreases simultaneously as depicted in Figure 3(c), resulting in a decrease in capacitance. Mathematically, a parallel plate capacitance can be expressed as per equation (4), as follows:

$$C = \varepsilon\,A/T \tag{4}$$

Where: $\varepsilon$, $A$, and $T$ are the dielectric constant, area, and thickness of piezoelectric layer sandwiched between the common and the outer electrode,

respectively.
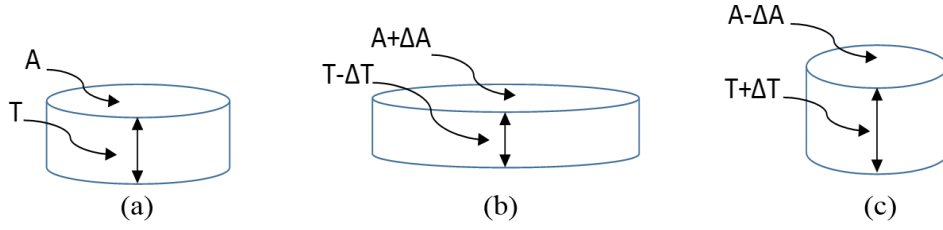


Figure 3: Illustration of piezoelectric materials response to applied electrical field: (a) unbiased disk, (b) anti-parallel and (c) parallel biasing schemes.

## 2.3 Piezoelectricity for Cardiac and Respiration Cycles

Piezoelectric sensors have been in use for several years in the field of respiration and cardiac signal acquisition. As an example, an in-house incorporated piezoelectric Bluetooth-enabled sensor and another commercially available respiration sensor (from Zephyr/USA), as shown in Figure 4, have been used to collect the chest response with and without breathing simultaneously. The Bluetooth-enabled systems allow collecting the data in a relaxed and reliable manner rather than using wiring and cables.

The piezoelectric sensor incorporates PZT materials with dimensions: 46 mm in length, 20 mm in width, and 0.26 mm in thickness with composition of PZT [144]. Figure 5 summarizes the measured responses using both sensors. The recorded signals in Figure 5 are up to 80 seconds and show a smooth variation in the piezoelectric; meanwhile, the Zephyr response at certain time points shows non-smooth variations. Figure 5 depicts the holding breath interval from 55 to 75 seconds. The Zephyr sensor response exhibits approximately linear behavior, while the piezoelectric sensor produces a strain of cycles that are conformally mapped with the cardiac mechanical

physiology. The utilized piezoelectric transducer exhibits reliable responses in both holding breath and respiration modes.
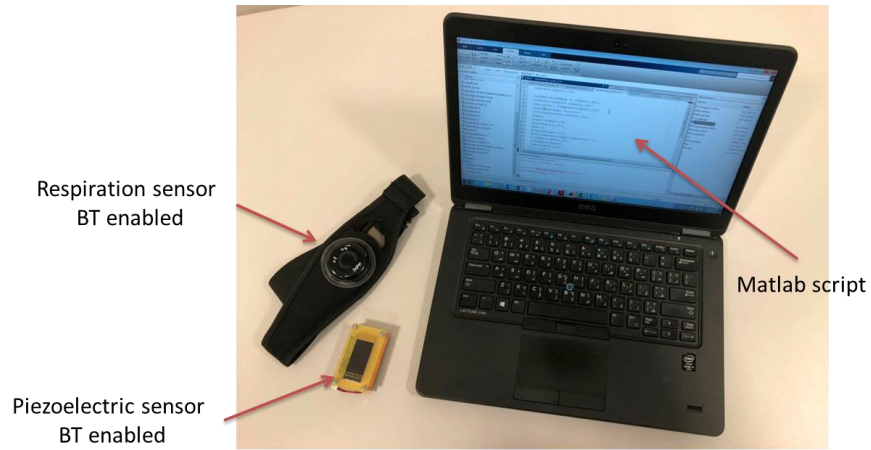


Figure 4: Employed experimental setup for piezoelectric sensor to collect chest signals
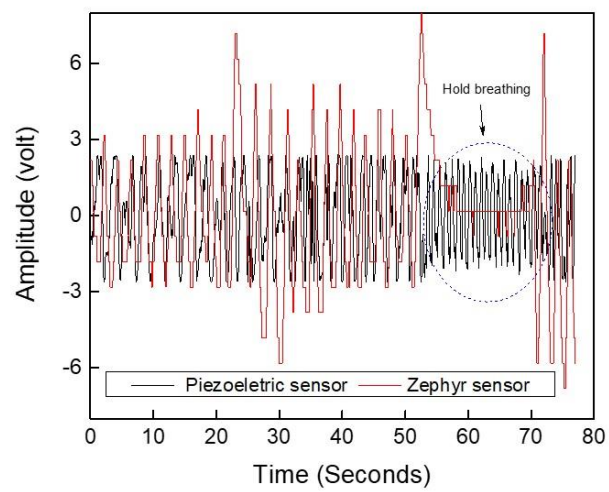


Figure 5: Measurements using piezoelectric sheet sensor and Zephyr sensor

## Chapter 3: Extraction of Piezoelectric Constants

The piezoelectric materials are incorporated in a smart structures to exhibit specific functionality. The activity of piezoelectric material dimension and electrical properties can be changed with an applied stress. These variations are translated to a change in the capacitance of the structure. This work takes a close look at the use of the capacitance-voltage measurements for extraction of double piezoelectric thin film material deposited at the two faces of a flexible steel sheet. The piezoelectric thin film materials have been deposited using the radiofrequency (RF) sputtering techniques. A Gamry analyzer Reference 3000 was used to collect the capacitance-voltage measurements from both layers. The developed algorithm extracts directly the piezoelectric coefficients knowing the film thickness, the applied voltage, and the capacitance ratio. The capacitance ratio is the ratio between the capacitances of the film when the applied field is antiparallel and parallel to the polling field direction, respectively. The method has been calibrated using a piezoelectric bulk ceramic and validated by comparing the result with the reported values in the literature. The extracted values using the current approach match well the values extracted by other existing methods.

## 3.1 Current Approach

In previous research [138, 139], Al Ahmad et al. have presented a new method of measuring piezoelectric thin film's vertical extension by utilizing the CV approach. This approach has received attention, and several studies have commented and elaborated on its advantages and disadvantages [145, 146]. Many researchers consider the reported CV method to be the easiest and quickest to provide results. This method

does not require sample preparations as in other methods, which make it also cheaper. In this work, the piezoelectric coefficients have been extracted by a new algorithm using the CV method and applied to a proposed piezoelectric structure. The development of advanced piezoelectric structures that incorporate two piezoelectric layers sandwiching a flexible metallic sheet call for further optimization and enhancement of the current existing characterization methods.

The application of DC field opposite to the polled field will result in the contraction of the layer thickness and expansion in the area, hence the capacitance is expressed as per equation (5):

$$C_{\downarrow\uparrow} = \varepsilon(A + \Delta A)(T - \Delta T)^{-1} \tag{5}$$

Where $\Delta A$ and $\Delta T$ are the variation in area and thickness, respectively. Meanwhile, the application of DC field parallel to the polled field will result in the contraction of the layer area and expansion in the thickness, hence the capacitance is expressed as per equation (6):

$$C_{\uparrow\uparrow} = \varepsilon(A - \Delta A)(T + \Delta T)^{-1} \tag{6}$$

Dividing (5) over (6), yields:

$$C_r(T - \Delta T)(T + \Delta T)^{-1} = (A + \Delta A)(A - \Delta A)^{-1} \tag{7}$$

Where Cr= C↓↑/C↑↑. Equation (7) connects the change in capacitance ratio with the change in dimension due to the piezoelectric effect. With the help of $(1 + x)^n = 1 + nx$, yields:

$$C_r(1 - 2\Delta T/T) = (1 + 2\Delta A/A) \tag{8}$$

Equation (8) correlates the changes in capacitance ratio to both changes in thickness and area.

It is worth mentioning that the deposition process of both layers may end up with different thicknesses and dielectric constants, as they are deposited sequentially. To overcome such discrepancies, the variation in areas, thicknesses, and dielectric constants are expressed in terms of applied electric field, rather than the applied voltage. By this, the geometrical variations and change in dielectric constants will be normalized. The variation in thickness and area in terms of applied electric field (E) can be expressed as follows [147]:

$$\pm\Delta T/T = \pm d_{33}E \tag{9}$$

$$\pm\Delta A/A = \pm 2d_{31}E + (d_{31}E)^2 \tag{10}$$

Where $d_{33}$ and $d_{31}$ are the longitudinal and transversal piezoelectric voltage constants, respectively. As revealed from (9), the variation in thickness exhibits a linear relationship with the applied field, and from (10) the variation in area exhibits a quadratic relationship with the applied field. Substituting (9) and (10) into (8), produces:

$$C_r - 2C_r d_{33}E = 1 + 4d_{31}E + 2(d_{31}E)^2 \tag{11}$$

Rearraning (11) for $d_{31}$, assuming $d_{33} = 2d_{31}$ yields:

$$2E^2 d_{31}^2 + (4EC_r + 4E)d_{31} + (1 - C_r) = 0 \tag{12}$$

Solving equation (12) for $d_{31}$, yields:

$$d_{31} = \left(-(C_r + 1) \pm \sqrt{C_r^2 + 2.5C_r + 0.5}\right)E^{-1} \tag{13}$$

Equation (13) states that there are two possible solutions, nevertheless, if the materials exhibit no piezoelectric effect, $Cr$ is equal to 1 and $d_{31}$ is equal to zero. Hence the solution should read:

$$d_{31} = \left( -(C_r + 1) + \sqrt{C_r{}^2 + 2.5C_r + 0.5} \right) E^{-1} \qquad (14)$$

The significant of (14) is that it can solve for $d_{31}$ without any required knowledge and information about the change in dielectric constant or any other variations. The only needed parameter is the thickness of the sputtered thin film. Hence, for a given piezoelectric film, after the polling process, the capacitances recorded correspond to specific voltage value with negative and positive polarities. Then the electric field ($E$) and capacitance ratio ($Cr$) are computed.

It is worth mentioning that the assumed condition $d_{33} \approx 2d_{31}$, can be replaced by a general one $d_{33} = xd_{31}$, where $x$ can assume its values between 1 and 3. Furthermore, almost 95% of the published literature in PZT-based piezoelectric materials has reported numerical values for $d_{33}$ and $d_{31}$; accordingly they can be approximated so that $d_{33} \approx 2d_{31}$. Indeed, for the PZT based materials, the domain structure of the grains has a strong influence on this ratio ($d_{33}/d_{31}$).

## 3.2 Sample Preparation

To demonstrate the current approach, a thin piezoelectric film was deposited on both sides of a steel sheet using the sputtering technique. The deposition conditions are listed in Table 2. The film post-annealing process was done at 700 ℃ for one hour. The thickness of the employed steel flexible sheet is of 50 μm, and the thickness of the

deposited piezoelectric layers on both steel sides was measured to be 2.41 μm. Figure 6 illustrates the stack composed of thin metallic steel sheets coated from both sides with noble materials PLT/Pt/Ti as a seeding layer for the deposition of the piezoelectric thin film materials layers on both faces of the steel. As illustrated in Figure 6, the shim layer is a flexible steel sheet which acts as a common electrode. Furthermore, both outer surfaces of PZE1 and PZE2 are coated with Al metallization to form electrical contacts. The film polling was conducted at room temperature with the application of 250 kV/cm for 20 minutes. The CV measurements were conducted between the metallic shim and the outer electrical electrodes.
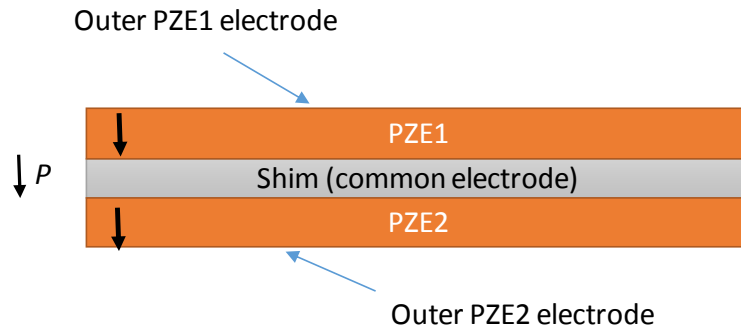


Figure 6: Illustration of double piezoelectric layers (PZE1 and PZE2) sandwiching a metallic sheet (shim) with polling directions (↓P)

Both layers were polled in the same direction, hence, for identically applied voltage polarities applied across them, their thicknesses will either increase or decrease simultaneously. Meanwhile, if the applied voltages polarities are opposite to each other, one layer will increase in thickness and the other layer thickness will decrease.

To assess the efficiency of the fabrication process, XRD measurements were conducted for the steel flexible sheet before PZT deposition (blank) and for the flexible sheet with a PZT deposited over steel (coated). Figure 7 represents the XRD

measurements, the filled circle represents the diffraction peaks of the steel flexible sheet, and the open circles represent the diffraction peaks of the PZT deposition layer on the flexible steel sheet. Clearly, the existence of multiple peaks stimulates the distribution of the peaks along the angle of orientation, revealinng that the PZT deposition quality is high and the sample does not have disordered materials.
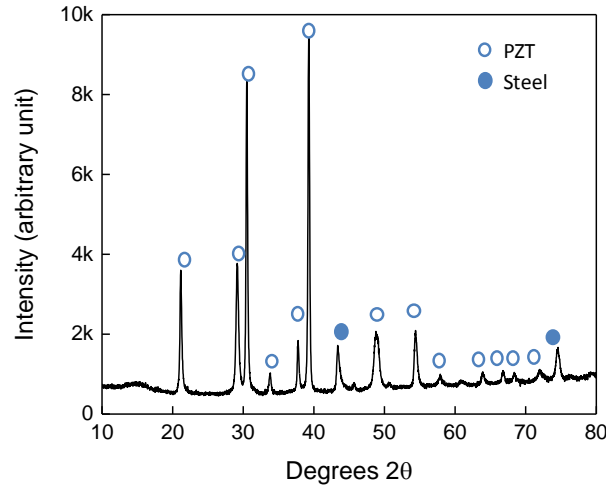
Figure 7: XRD measurements of the fabricated PZT layer

Table 2: PZT thin film deposition conditions

|  | Ti | Pt | PLT | PZT |
| --- | --- | --- | --- | --- |
| Deposition temp [℃] | 500 | 500 | 650 | 700 |
| Sputtering Pressure [Pa] | 0.8 | 0.5 | 0.5 | 0.5 |
| RF power [W] | 80 | 100 | 150 | 90 |
| Ar/O2 [sccm] | 20/0 | 20/0 | 19.5/0.5 | 19.5/0.5 |
| Deposition time [min] | 6 | 8 | 15 | 300 |

## 3.3 Calibration Method

To further calibrate the proposed method, PZT unclamped bulk ceramic with thickness 0.24 mm has been utilized. The CV measurements are depicted in Figure 8. The measured $d_{31}$ using Berlincourt meter is 250 pm per volt of this unclamped sample. The extracted $d_{31}$ piezoelectric voltage constant using equation (14) yields 190 pm per volt. The current method is corrected by multiplying equation (14) with a factor (4/3), to correct the discrepancy between measured and extracted values. Therefore the modified equation reads:

$$d_{31} = (4/3)\left(-(C_r + 1) + \sqrt{C_r^2 + 2.5C_r + 0.5}\right)E^{-1} \tag{15}$$
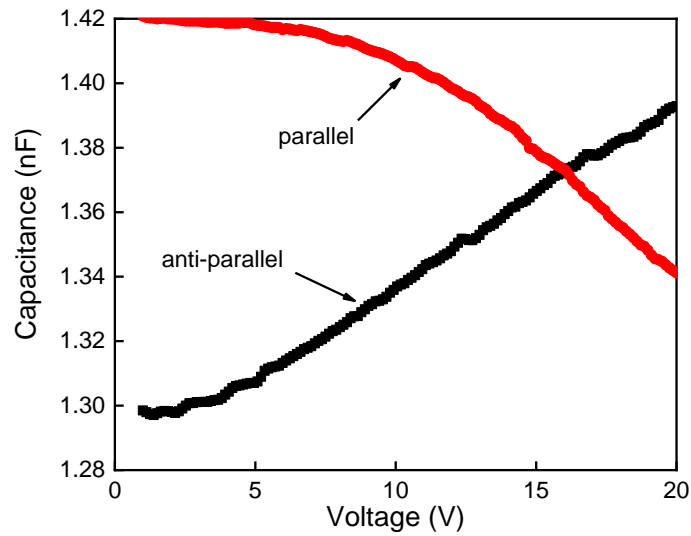


Figure 8: Measured CV of bulk sample

**3.4 Results and Discussion**

The electrical measurements were taken using a Gamry Reference 3000 analyzer. Capacitances versus frequency measurements (at zero bias) were conducted to determine the frequency range and its self-resonance frequency. The capacitance shows a smooth response over the frequency as displayed by Figure 9. The measurements were taken along frequency variations in the range of 1-80 kHz. A dc voltage was applied to both layers for capacitance versus frequency at +3 volt DC bias (anti-polarization), and at -3 volt DC voltage bias (parallel to polarization).
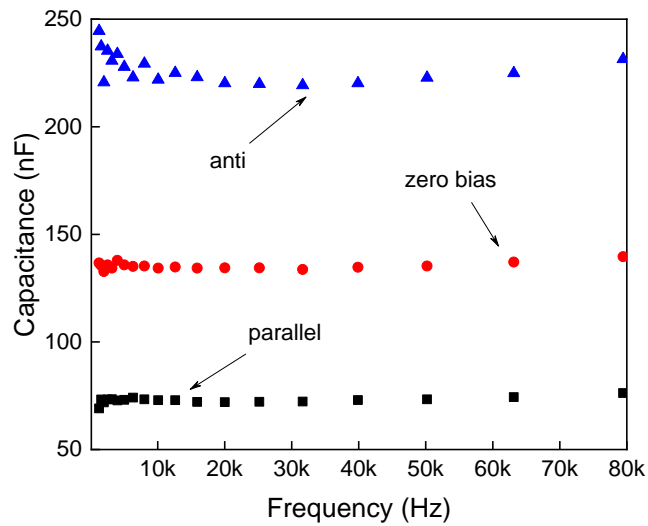


Figure 9: Capacitance versus frequency measurements for unbiased (at zero volts), anti-parallel (at +3 volt) and parallel biasing (at -3 volt)

Figure 8 and 9 show that when the applied voltage is anti-parallel to the polling direction of PZT material, the values of the measured capacitance increases with the frequency as it reaches around 230 nF. On the other hand, applying voltage parallel to the polling direction decreases the values of the measured capacitance slightly with the frequency and reaches around 75 nF. While in the zero biasing case, the capacitance measurements nearly stayed constant around the value 135 nF over the range of

frequencies. As anticipated, the applied voltage in either parallel or opposite to polling direction will cause a change in the dimension which is pronounced by the capacitance measurements.

The two layers were polled in opposite directions. Figure 10 shows the two piezoelectric capacitance voltage responses when the applied voltage is swept from -0.3 to +0.3 volts. For layer 1, the capacitance increased for the positive applied field as it was driven opposite to the polling field direction, meanwhile it decreased for the negative values as it was driven parallel to the polling field direction. On the contrary, for layer 2, the capacitance increased for the negative applied field as it was driven parallel to the polling field direction, meanwhile it decreased for positive values as it was driven opposite to the polling field direction.
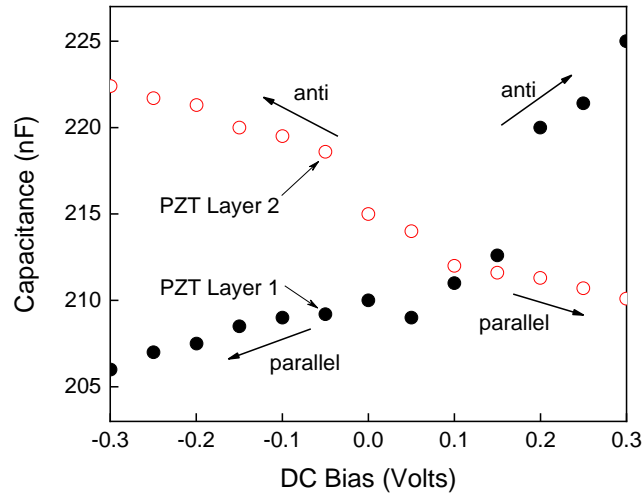


Figure 10: Simultaneous CV measurements of the two piezoelectric layers

With the help of equation (15) and the data presented in Figure 6, the extracted $d_{31}$ and $d_{33}$ piezoelectric voltage constants have been estimated and depicted in Figure 11. The applied electric field is of 1.25 volt per μm. The constants exhibit a smooth behavior over a wide frequency range. At a frequency of 40 kHz, $d_{33}$ and

$d_{31}$ constants read 284 and 142 pm per volt, respectively. These values are comparable with reported values in the literature for the same thin film thickness [148].
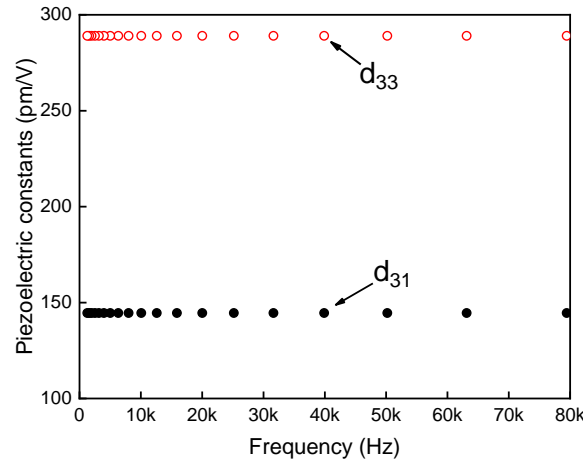


Figure 11: Extracted piezoelectric voltage constants using (15)

Equation (15) along with CV measurements presented in Figure 10 have been used to extract the piezoelectric constants of both layer 1 and layer 2 of the stack shown in Figure 6. The estimated mean values of values for $d_{31}$ of layers 1 and 2 are 125 and 130 pm per volt, respectively. Furthermore, the variation in the capacitance incorporating piezoelectric materials due to the applied voltage can be generated either by the dielectric constant voltage dependency and/or from the expansion/contraction in the dimensions of the polled material.

Figure 12 revealed that the change in the polarization due to the change in electric field is equal to 1.6 C/cm$^2$. Hence, the equivalent capacitance change from this change in polarization is 0.6 pF. Therefore, 1% of the measured capacitance change is due to dielectric constant voltage dependency while 99% of this change is referred to the variations of sample dimensions due to the piezoelectric effect. The piezoelectric

constant ($e_{31},f$) is then estimated to be -3.8 C/m$^2$. The dielectric constant of the film is computed to be 240 on average.
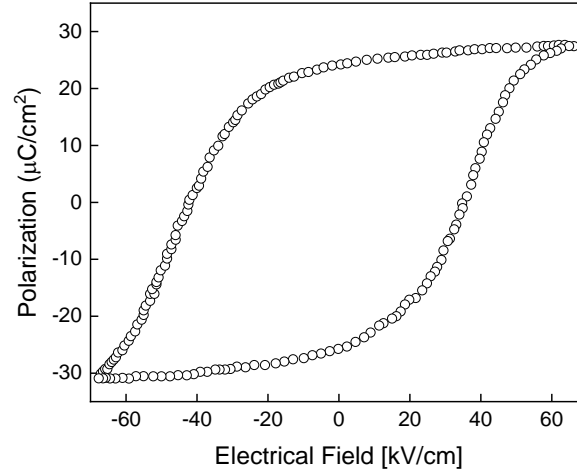


Figure 12: Polarization curve for the deposited film above steel sheet

## 3.5 Summary

The characterization of piezoelectric constants relevant to a specific application will enhance their use. This work contributes to the development of an innovative methodology to determine the piezoelectric constants. The piezoelectric material should be incorporated as a capacitance dielectric material. An electric field is then applied to drive the film parallel and anti-parallel to the polling field direction. This is usually done by sweeping the voltage from negative to positive values. The variations in geometric dimensions and the corresponding dielectric constant of the materials due to the applied field will be reflected in the measured capacitance. The developed model requires only the pre-knowledge of the film thickness and automatically de-embeds the change in dielectric constant due to the applied stress. The proposed method has been calibrated using unclamped bulk PZT ceramic and

validated using conventional meters. The estimated and measured values are well

corroborated with each other. The proposed technique does not require any sample

heavy preparation steps, and provides a rapid response along with accurate estimation.

# Chapter 4: Noninvasive Piezoelectric Detection

Monitoring of vital signs plays a key role in the diagnosis of several diseases. Piezoelectric sensors have been utilized to collect a corresponding representative signal from the chest surface. The subject typically needs to hold his or her breath to eliminate the respiration effect. This work further contributes to the extraction of the corresponding representative vital signs directly from the measured respiration signal. The contraction and expansion of the heart muscles, as well as the respiration activities, will induce a mechanical vibration across the chest wall. This vibration can be converted into an electrical output voltage via piezoelectric sensors. During breathing, the measured voltage signal is composed of the cardiac cycle activities modulated along with the respiratory cycle activity.

The proposed technique employs the principles of piezoelectric and signal-processing methods to extract the corresponding signal of cardiac cycle activities from a breathing signal measured in real time. All the results were validated step by step by a conventional apparatus, with good agreement observed.

In a previous work, Al Ahmad and Al Shareef proposed a noninvasive piezoelectric-based method to count the heart rate [138]. The piezoelectric sheet was placed on the chest. The mechanical activity of the heart causes the sheet to deform, which produces a voltage signal. A mechanical model was developed based on the corresponding electrical waveform. The main constraint here was that the signals were collected while the patient held his or her breath; thus, the method must be improved to eliminate the respiration constraint. In this thesis, a novel piezoelectric-based approach that allows for the extraction of cardiac cycle parameters from a breathing measured signal is investigated. During breathing, the measured voltage signal is

composed of the cardiac cyclic activities modulated along with the respiratory cyclic activity.

The proposed method utilizes the principles of the piezoelectric and convolution techniques along with Fourier transformation to extract the corresponding signal of the cardiac cycle activities from a breathing signal measured in real time.

In the following sections, the processes used to extract respiration, heart rate and blood pressure values will be discussed sequentially. These parameters are extracted directly from the output voltage of the piezoelectric sheet simultaneously.

## 4.1 Extraction of Respiration Rate

The physiological activities of lungs induce mechanical vibrations inside the chest wall [149]. Such vibrations are correlated with the respiration rate [150]. When a piezoelectric sheet is positioned on the exterior surface of the chest, such induced vibrations acts as a mechanical load on the piezoelectric sheet. The piezoelectric sheet correspondingly produces an electrical voltage signal that is correlated with the activities of lungs and heart [151].

Figure 13(a) displays the measured output voltage time domain signal collected using a piezoelectric sheet placed on top of the chest. The periodic signal has multiple peaks numbered from 1-8 over a 20 s time period. The peaks are conformally mapped to the lungs' performance. The volume of inlet air to the lungs, which is called the tidal volume, is correlated with the maximum peaks. The slope between the maximum peak (A) and minimum peak (B) reflects the exhalation process, while the slope between the minimum peak (B) and maximum peak (C) reflects the inhalation process of

breathing and applies to the remaining peaks. The peaks of the piezoelectric signal taken upon breathing were defined. The time span between each maximum peak and the next one, as well as between the bottom peaks, represents the breath cycle period ($B_c$). Figure 13(b) illustrates that the cycle period changes slightly from cycle to cycle, and in (c) the average breath cycle with standard deviation.
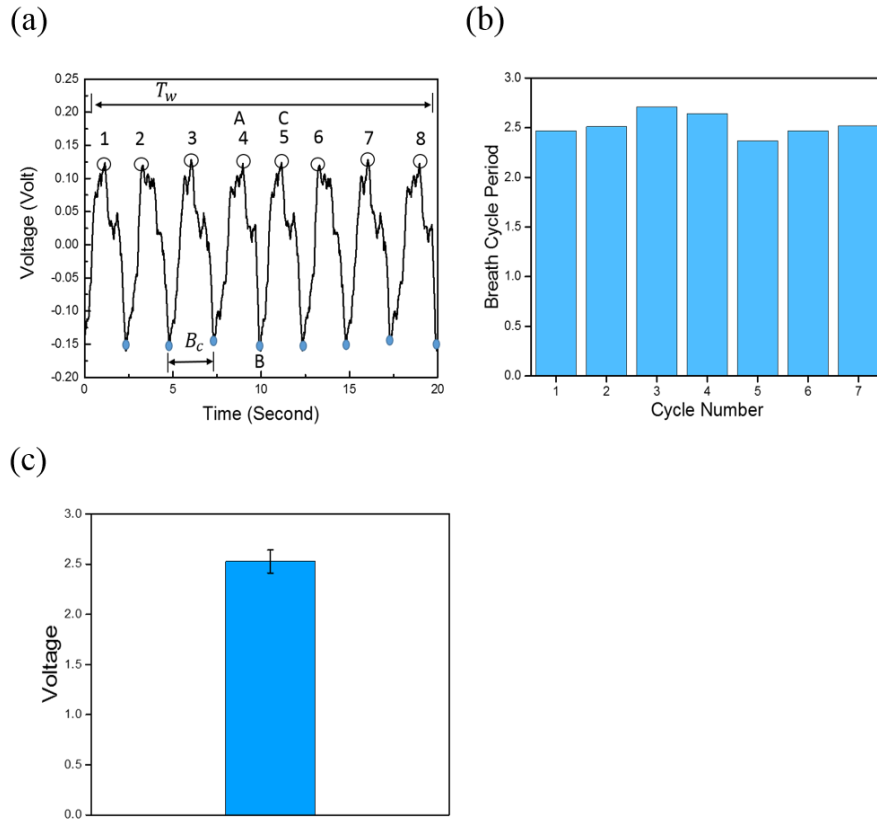


Figure 13: Extracting respiration rate (a) Output voltage measured using a piezoelectric sheet while breathing. (b) Changes in the breath cycle period over the cycles (c) The average cycle with standard deviation.

By taking the average of the cycles and then calculating the respiration rate per minute by dividing 60 over the time period of the averaged cycle, a respiration rate of 23.7 is obtained for the subject. The following expression was used to extract the respiration rate (breath per minute) from the piezoelectric signal:

$$RR = N^P \left(\frac{60}{T_w}\right) \tag{16}$$

Where $T_w$ is a selected period of time during which the signal is collected and $N^P$ is the number of positive peaks for the selected period of time. The period of breath cycle variation was considered by taking the signal over a selected period and then converting it to breaths per minute. Using equation (16) and the data presented in Figure 12(a), the calculated $RR$ was found to be 24 breaths per minute. In comparison, the measured rate found by counting the breaths taken in one minute was 23 breaths per minute, indicating an error of less than 5%.

## 4.2 Extraction of Heartbeat Rate

Heartbeat parameters are extracted from a holding-breath signal since this type of signal is a heart signal without the interference of the respiration effect. The signal was taken over a selected period of time using the same piezoelectric sensor placed on the left side of the chest, as shown in Figure 14(a). The measured piezoelectric signal is conformally mapped to the heart mechanical activities. There are three main heart actions, which are represented in the output piezoelectric signal in three regions. The first region reflects the atrial contraction and is marked by (A) in Figure 14(a). This region is generated due to the depolarization of the atrial fibers and aortic valve opening, which causes the contraction.

The second region represents the ventricular contraction and is represented as (B)–(D) in Figure 14(a). The ventricular contraction is generated due to the depolarization of ventricular fibers. This activation, along with the closing of the aortic valve, makes the ventricules contract. Thus, the stress of the heart is intensified by

ventricular depolarization in the ejection or contracting interval, which is between points (B) and (C). The aortic valves are then re-opened, and the repolarization of ventricular fibers is initiated to the relaxation point, represented by (D). Thus, the heart stress decreases until reaching point (D). Repolarizing the ventricular fibers will retrieve its actions and increase the heart stress to reach point (E) [152].
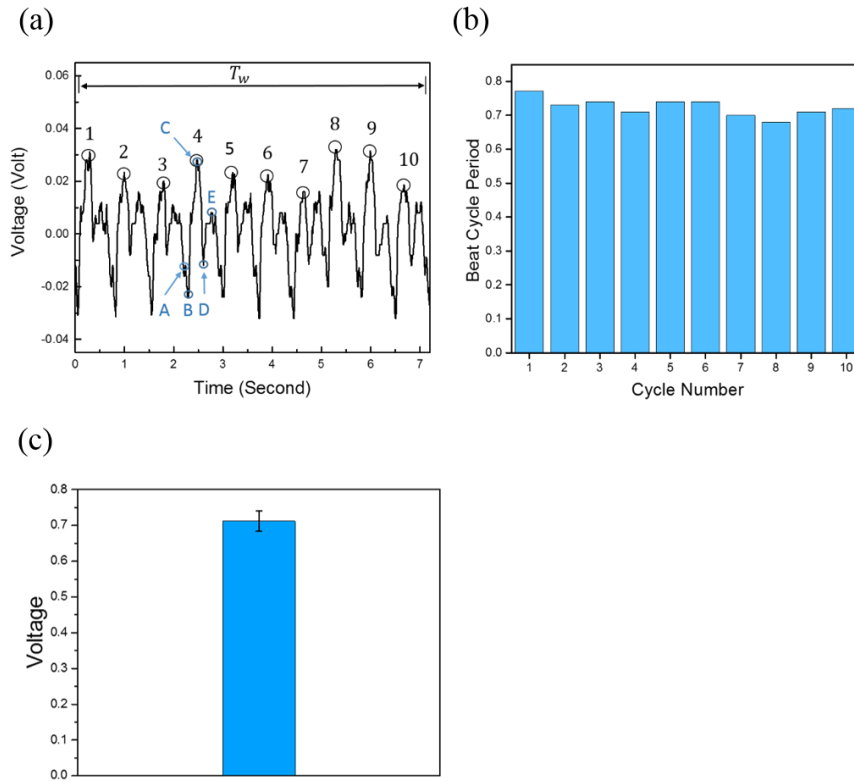


Figure 14: Extracting heart rate (a) Output voltage measured using a piezoelectric sheet while the patient held his or her breath. (b) Heartbeat cycle period changes over the cycles (c) The average cycle and standard deviation.

The peaks of the piezoelectric signal were defined. The time span between the maximum peaks or bottom peaks represents the beat cycle period. The heartbeat cycle period varies slightly from cycle to cycle, as shown in Figure 14(b). The average value of the time range of the cycles is shown in Figure 14(c) with the standard deviation. To extract the heart rate from the piezoelectric signal, the beat cycle peaks, denoted by

1-10 in Figure 14(b), were counted ($N^P$) over a selected period of time ($T_w$), and the following expression was employed:

$$HR = N^P \left(\frac{60}{T_w}\right) \tag{17}$$

Using equation (17) and the data presented in Figure 14(a), the calculated *HR* was found to be 83 beats per minute. In comparison, the measured rate found by counting the heart beats taken in one minute was 87 beats per minute, indicating an error of less than 5%.

## 4.3 Extraction of Blood Pressure Values

Another vital sign was extracted from the piezoelectric signals when the patient was holding his or her breath, namely, the blood pressure. When the signal was collected from the piezoelectric sheet, the systolic pressure (*SP*) and diastolic pressure (*DP*) were measured at the same moment conventionally using an electronic sphygmomanometer, or a blood pressure meter. The *DP* can be extracted from the heartbeat signal by mapping the *SP* from the conventional meter with the maximum value of the heartbeat signal. First, from the conventional meter readings, one can obtain:

$$\Delta P_m = SP_m - DP_m \tag{18}$$

Where $\Delta P_c$ is the difference between the $SP_c$ and $DP_c$ of the conventional meter. On the other hand, the maximum and minimum of the heartbeat signal collected from the piezoelectric signal while holding the breath are represented by *H* and *L*, respectively, as shown in Figure 15(a).

The difference between H and L is:

$$\Delta_o : \Delta_0 = H - L \tag{19}$$

The piezoelectric signal revealed that each 1 mv in the piezoelectric voltage signal corresponds to 1 mmHg in the conventional meter blood pressure readings.

The average value of the maximum peaks ($H_{av}$) corresponds to the highest reading value in the conventional meter ($SP_m$). The same applies to the cycle level value of the piezoelectric signal ($H_{cycle}$) and blood pressure value ($SP_{cycle}$). The following statements relate the piezoelectric signal to the blood pressure values:

$$H_{cycle} = (SP_{cycle} H_{av})/SP_m \tag{20}$$

$$L_{cycle} = H_{cycle} - \Delta_{v\_cycle} \tag{21}$$

For the entire holding-breath signal, the average $\Delta_o$ was found to be 0.0527. The average $H$ was 0.0246, the average $L$ was 0.0281, and $\Delta P_c$ was 48. From the previous equations, the $SP$ and $DP$ were extracted from each cycle of the hold-breathing signal, as shown in Figure 15(b). The average extracted $SP$ was 112, and the average $DP$ was 64. Figure 15(c) shows the average values of the systolic and diastolic pressure along with the standard deviation over the selected time range. In comparison, the values from the conventional meter for the $SP$ and $DP$ were 112 and 64, respectively.

(a)

(b)

(c)
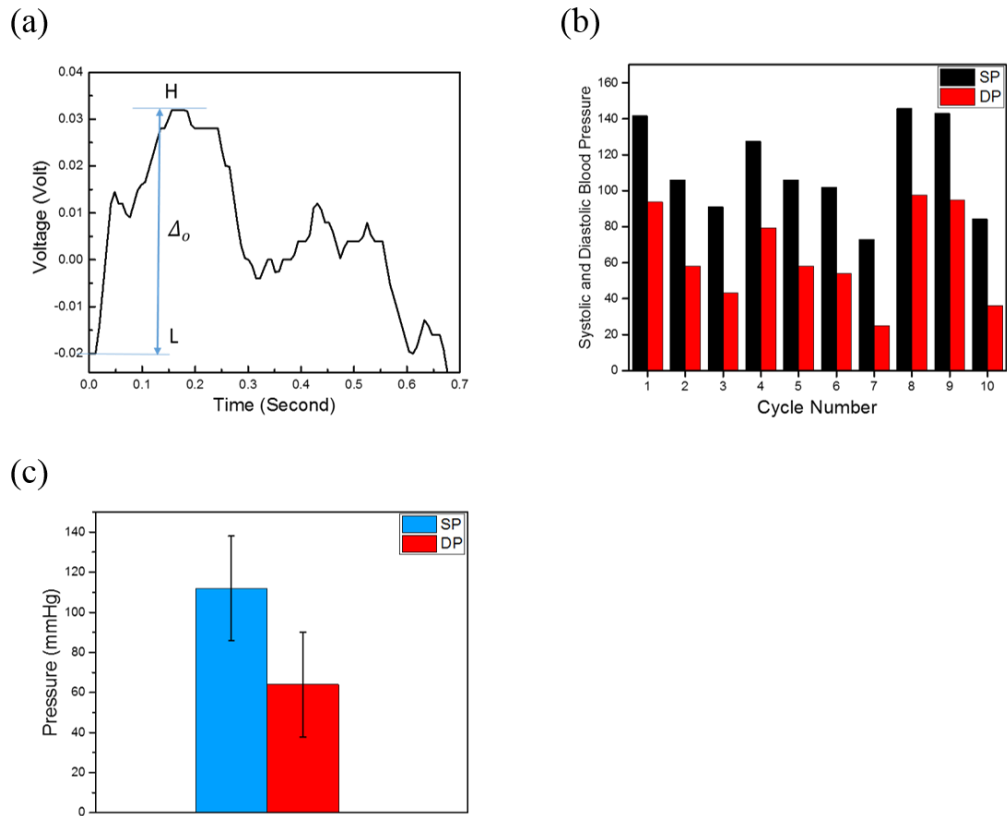


Figure 15: Extracting blood pressure (a) A cycle of the signal obtained while the patient was holding his or her breath, labeled with H and L peaks. (b) The variations of the SP and DP extracted from each cycle (c) The average cycles and standard deviation.

A comparison of the output voltages signals in Figures 13(a) and 14(a) illustrates that the breathing signal is three times larger in amplitude than the hold-breathing signal; the produced electrical voltage corresponds to only cardiac cycle contraction and expansion activities. Meanwhile, during the breathing mode, the generated electrical voltage is due to both heart muscle and lung activities simultaneously. The hold-breathing signal exhibits a higher frequency than the breathing signal. The frequency of the latter signal represents the respiration rate, whereas the frequency of the former signal represents the heart rate. The heart rate is always higher than the respiration rate because the lungs normally expands and contracts up to 20 times a minute to supply oxygen to be distributed throughout the

body and expel carbon dioxide that has been created throughout the body [153]. Meanwhile, the heart muscle expands and contracts up to 100 times a minute to supply blood the whole body [154].

In the next upcoming sections, the RR, HR and BP values will be extracted directly from the corresponding output signal of respiration via signal-processing methods.

## 4.4 Extraction of the Cardiac Signal from the Respiration Signal

As illustrated previously, the heart rate can be easily extracted from the piezoelectric signal under the hold-breathing situation. However, this extraction method is not practical when asking the patients to continue to hold their breath. Thus, accurately extracting the entire heartbeat signal from the respiration signal becomes critical. The significance of the heartbeat signal involves the ability to extract its multiple vital signs, such as the heart rate, SP and DP.
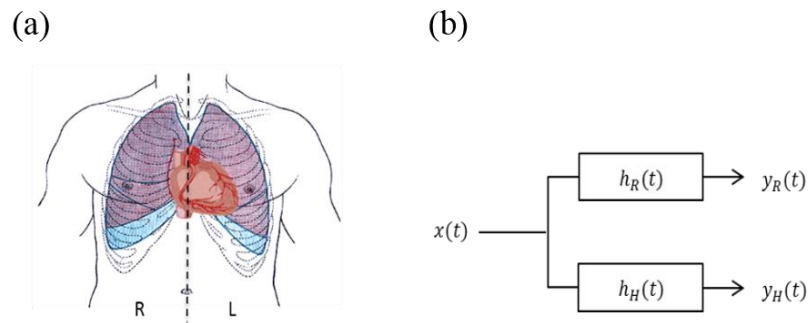


Figure 16: Schematic illustrations: (a) human upper body schema (heart, lungs, and thorax); chest is divided into the left side (L) and right side (R). (b) System representation and modeling. The excitation signal is represented by x(t), the respiration signal.

This section proposes a pre-processing method for removing the respiration-related component from the signal of a piezoelectric sensor located on the chest. The schematic representation and system modeling of the current approach are illustrated in Figures 16(a) and (b), respectively. Figure 16(a) illustrates the left and right sides of the human chest, within which both the lungs and heart are shown.

Based on the causality principle, the presented system model in Figure 16(b) is proposed to establish the relationships among the different signals. The chest wall exhibits two impulse responses according to whether it is in hold-breathing ($h_R(t)$) or breathing mode ($h_H(t)$). Based on this model, one can argue that both breathing and hold-breathing actions are generated from the same excitation signal source. This excitation signal can be represented by a two-level minimum and maximum threshold function. The hold-breathing model is activated when a minimum threshold is assumed, whereas the breathing mode is activated when its maximum value is assumed. From the modeling shown in Figure 16(b) and using convolution theory [155], $y_R(t)$ and $y_H(t)$ are expressed as:

$$y_R(t) = x(t) * h_R(t) \tag{22}$$

$$y_H(t) = x(t) * h_H(t) \tag{23}$$

Where "*" represents the convolution operator. $h_R(t)$ and $h_H(t)$ represent the chest wall impulse responses under the breathing and hold-breathing modes, respectively. These responses depend on several parameters, namely, the chest wall thickness and human health conditions. The Fourier transform [156] of (22) and (23) yields

$$Y_R(f) = X(f)H_R(f) \tag{24}$$

$$Y_H(f) = X(f)H_H(f) \tag{25}$$

Where $Y_R(f)$, $Y_H(f)$, $X(f)$, $H_R(f)$ and $H_H(f)$ are the corresponding Fourier transforms of $y_R(t)$, $y_H(t)$, $x(t)$, $h_R(t)$ and $h_H(t)$, respectively. The objective is to extract $y_H(t)$ directly from $y_R(t)$. Dividing (25) over (24) yields

$$Y_H(f) = Y_R(f) \left( \frac{H_H(f)}{H_R(f)} \right) \tag{26}$$

Rearranging (26) and taking the inverseOurier transform yields

$$y_H(t) = F^{-1} \left[ \frac{H_H(f)}{H_R(f)} \right] * y_R(t) \tag{27}$$

Hence, (27) represents the hold-breathing time domain extracted signal from the measured respiration signal. For further simplification, $\Gamma(t)$ is introduced as follows:

$$\Gamma(t) = F^{-1} \left[ \frac{H_H(f)}{H_R(f)} \right] \tag{28}$$

As long as there are no changes in the physiological status of the subject health in terms of lungs, cardiac diseases and dramatic weight change, $\Gamma(t)$ remains an invariable time domain response. Otherwise, $\Gamma(t)$ will vary accordingly and should be recomputed. Furthermore, since both cardiac and respiratory parameters are expressed per minute, the averaging of the hold-breathing and breathing cycles is introduced. Moreover, to count for the invariable time domain response, the initial measured and averaged cycles for the breathing ($H_{R0}(f)$) and hold-breathing ($H_{H0}(f)$) responses are used to compute $\Gamma_0(t)$ as follows:

$$\Gamma_0(t) = F^{-1} \left[ \frac{H_{H0}(f)}{H_{R0}(f)} \right] \tag{29}$$

While fabricating, thicknesses of the deposited piezoelectric material defers from device to another. To overcome this issue, the initial measurements are done once at the beginning to find the $\Gamma_0(t)$. These measurements and calculations that are perfomed at the initial stage are used to calibrate the sensor.

## 4.5 Measurements and Analysis

A set of experiments have been designed and conducted to explore, investigate and validate the developed theoretical approach.

### 4.5.1 Computation of the Chest Impulse Response

To execute the proposed algorithm, because the periodicities of the hold-breathing and breathing cycles are not identical and differ slightly from each other within the same mode, an average cycle for each mode is first computed. Figures 17(a) and (b) illustrate the average cycle for the breathing and hold-breathing modes, respectively. This averaging is recommended to overcome the slight change in periodicity of the cycles within the same mode.

To proceed further, the average breathing cycle has been scaled down in time to have the same period as for the average holding-breath cycle, as depicted in Figure 17(c). This scaled-down process is important to proceed with the calculations, as both signals should have the same time length. The variability in respiration cycle lengths and heartbeat intervals when calculating the average signal has been considered along with the direct impact of the variation in the respiration time scale on the frequency response scale. Meanwhile, the average cycle of the hold-breathing signal is interpolated to increase the time points, as displayed in Figure 17(d). Then, the

corresponding frequency domain signals for the average cycles are computed using the Fourier transform. Their magnitudes versus frequency are plotted in Figures 18(a) and (b).

Recalling equations (27) and (28), the $\Gamma_0(f)$ function can be computed directly from $Y_{H0}(f)$ and $Y_{R0}(f)$ as follows:

$$\Gamma_0(f) = Y_{H0}(f)/Y_{R0}(f) \tag{30}$$

Where $Y_{H0}(f)$ and $Y_{R0}(f)$ are the corresponding frequency domain signals for the average hold-breathing and breathing mode cycles, respectively. Figures 18(c) and (d) represent the frequency and time domain responses of $\Gamma_0(f)$, respectively, which will be utilized in the next subsection to compute the corresponding hold-breathing signal.
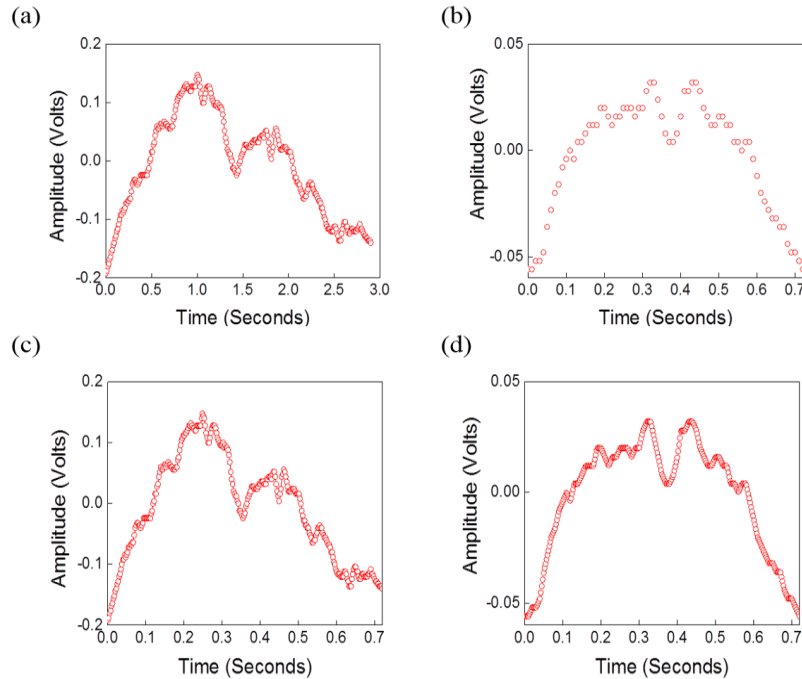


Figure 17: Measured average signals cycles: (a) average breathing of three constitute cycles and (b) average hold-breathing cycle signals of eight constitute cycles, respectively; (c) scaled-down average breathing cycle; (d) interpolated average hold-breathing cycle.

**4.5.2 Cardiac Cycle Extraction**

To reconstruct the corresponding hold-breathing signal from an instantaneous measured breathing signal, (27) can be reformulated as follows:

$$y_H(t) = F^{-1}\left[\left(\frac{H_{H0}(f)}{H_{R0}(f)}\right) Y_R(f)\right] \tag{31}$$

Using equation (31), an instantaneous cycle can be reconstructed by multiplying the Fourier transform of an instantaneously measured breathing cycle with the predefined chest impulse response, $\Gamma_0(f)$, computed in the previous subsection. The instantaneous hold-breathing cycle ($y_H(t)$) can then be extracted by finding the inverse Fourier transform of this multiplication.

Figure 19(a) represents an instantaneously measured cycle with a respiration rate of 25 breaths per minute. The corresponding reconstructed hold-breathing cycles are shown in Figure 19(b). The corresponding heart rate is computed to be 85 beats per minute. The reconstructed signal cycles are superimposed with the averaged measured hold-breath cycles in Figure 19(b). As revealed by comparing both signals in Figure 19(b), the algorithm reproduces the hold breath signal cycles with high accuracy.

(a)

(b)

(c)

(d)
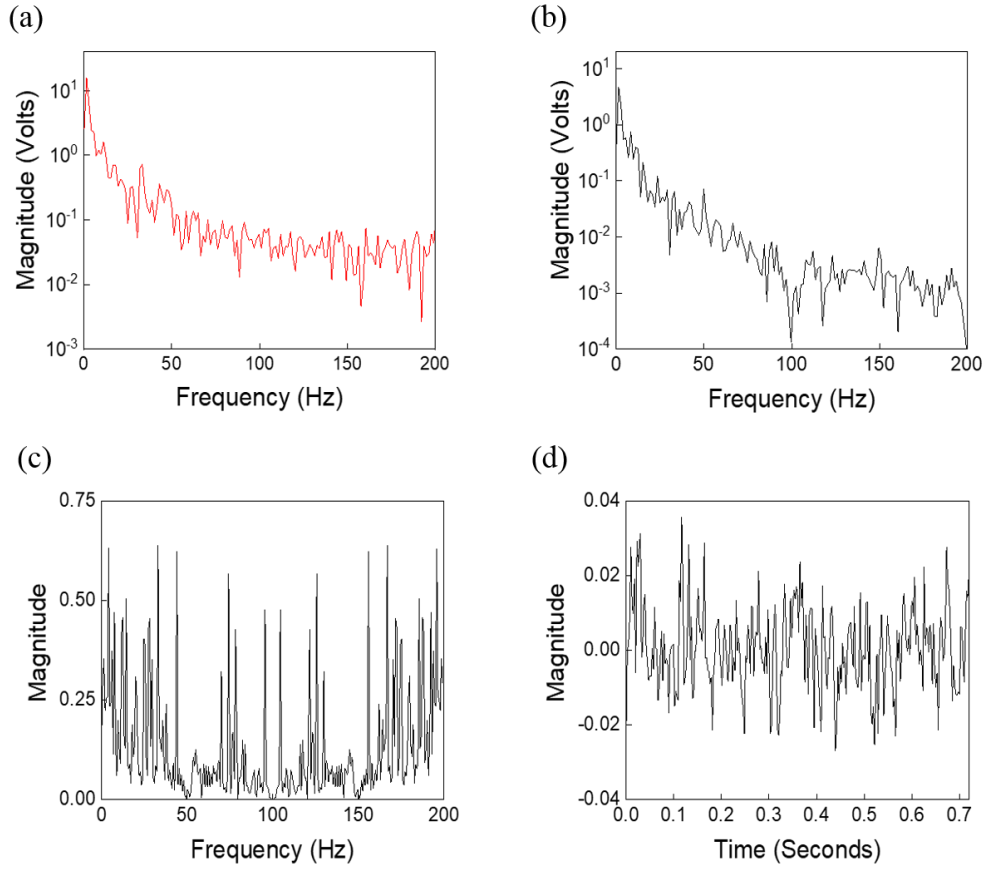


Figure 18: Gamma time and frequency domain signals: (a) magnitudes of the frequency domains of the average hold-breathing (Y_H0 (f)) and (b) breathing (Y_R0 (f)) cycle signals; (c) computed frequency and (d) and time domain signals of $\Gamma\_0$ (f).

## 4.6 Validation

For further validation; the breath and hold-breathing signals were collected from different human subjects using the Bluetooth-enabled piezoelectric system. In addition to that, the six subjects corresponding vital signs: respiration rate, heartbeat rate, and pressure pulse were measured using the conventional equipment.

Table 3 summarizes the measured vital signs using conventional equipment and methods along with weight, height, age and subject's gender. Figure 20 shows the average respiration cycles along with the corresponding hold-breathing signal

superimposed with the averaged measured hold-breathing cycles of selected cases. Figures 20(a), (c) and (e) are the instantaneously measured breathing cycles, and (b), (d) and (f) are their corresponding extracted hold-breathing corresponding cycles superimposed with the average measured hold-breathing cycles.

Table 3: Measured parameters for using conventional meters*

| Case | W | H | RR | PP | HB | Age | Gender |
|------|-----|------|-----|-----|-----|-----|--------|
| 1 | 55 | 1.61 | 21 | 35 | 74 | 26 | F |
| 2 | 40 | 1.53 | 26 | 32 | 83 | 28 | F |
| 3 | 51 | 1.62 | 18 | 29 | 65 | 29 | F |
| 4 | 50 | 1.54 | 27 | 32 | 70 | 33 | F |
| 5 | 58 | 1.59 | 23 | 31 | 79 | 27 | F |
| 6 | 53 | 1.62 | 21 | 38 | 60 | 25 | M |

* Where; *W*: weigh in kg; *H*: height in meter; *RR*: respiration rate in breath per minute; *PP*: pulse pressure in mmHg; *HB*: heartbeat in beat per minute.
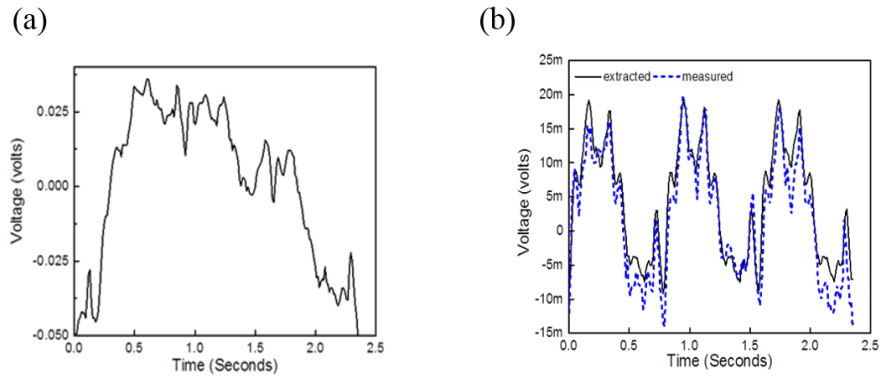


Figure 19: Extraction of the hold-breathing signal: (a) instantaneous measured breathing cycle and (b) corresponding constructed hold-breathing cycles
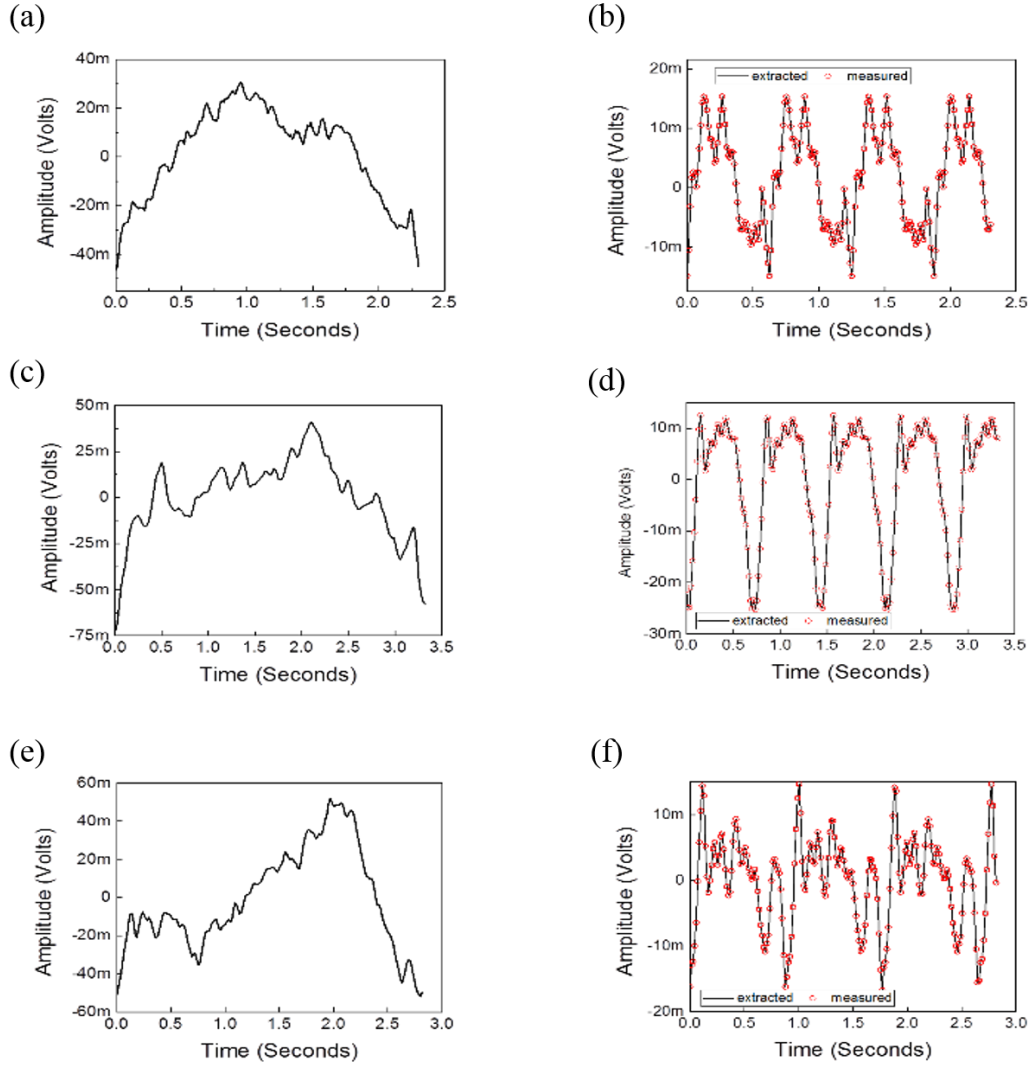
Figure 20: Selected cases: (a), (c) and (e) are the instantaneously measured breathing cycles, and (b), (d) and (f) are the corresponding constructed hold-breathing cycles superimposed with the average measured hold-breathing cycles.

Now, the corresponding *RHB* and *PP* parameters have been estimated from the signal represented in Figure 8. The current approach has been successfully employed to extract the hold breathing signals. Figures 20(b), (d) and (f) revealed that measured and extracted are well cooperated with each other. The error in regeneration of the holding-breath signal is very negligible. With the algorithms presented in reference [20]; the corresponding computed parameters are summarized in Table 4.

Table 4: Extracted parameters from reconstructed hold breathing cycles*

|  | **Estimated** | | | **Error (%)** | | |
|---|---|---|---|---|---|---|
| **Case** | RR | HB | PP | $E_{RR}$ | $E_{HB}$ | $E_{PP}$ |
| **1** | 24 | 66 | 27 | 14 | 10 | 22 |
| **2** | 26 | 75 | 29 | 0.0 | 9 | 9 |
| **4** | 20 | 75 | 32 | 11 | 15 | 10 |
| **5** | 26 | 66 | 21 | 3.0 | 5 | 34 |
| **6** | 30 | 80 | 30 | 30 | 1 | 3 |
| **7** | 20 | 60 | 27 | 4.0 | 0 | 28 |
| **Average error (%)** | | | | 10 | 7 | 18 |

*$E_{RR}$, $E_{HB}$ and $E_{PP}$ are the errors in *RR* rate, *HB* rate and *PP*, respectively.

The hold-breathing cycles extracted from the relevant respiration signals are identical to the measured hold-breathing cycles. Hence, the error of this extraction process is almost negligible, which proves the validity of the algorithm. The exact location of the sensor affects the transfer functions, and the appropriate position has been optimized experimentally. The left side of the chest is the optimal position for the piezoelectric sheet to extract the hold-breathing signal. Nevertheless, the right side of the developed algorithm can extract the hold-breathing signal from the piezoelectric sheet placed on the right side of the chest, which is beneficial for patients with special conditions.

**4.7 Discussion**

The main application of the current work is the monitoring of multiple vital signs of patients, such as the respiration rate from the piezoelectric signal, heart rate, and blood pressure from the extracted heart beat signal. The advantage of the algorithm is that it does not require the patient to hold his or her breath while measuring and is improved compared to the existing algorithm; the proposed algorithm is able to measure a patient's heart rate and blood pressure using one small piezoelectric sheet while moving normally. Being able to measure multiple vital signs from one piezoelectric sheet makes the monitoring easier and more comfortable for patients, with fewer wiring complications. Moreover, the proposed method can extract the heart rate signal from the right side of the chest for special cases where the patient cannot tolerate electric monitors on top of the heart position.

Sullivan et al. [157] proposed a system composed of piezoelectric sensors and signal conditioning circuits and signal processing to extract multiple vital signs. They used sensors attached to the body of a person to detect signals, including mechanical, thermal and acoustic signals reflecting cardiac output, cardiac function, internal bleeding, respiratoration, pulse, apnea, and temperature. For noise reduction, they have used a separate piezoelectric sensor that was not attached to the person was used. Instead, the sensor was exposed to the environmental acoustic and vibration signals, while the sensor attached to the body was exposed to the environment as well as the body signals. Subtraction of one input from the other allows for noise reduction and yields only the signal of the body using initial measurements as control signals. They described that some of those measurements were related to heart rate measurements in the absence of respiration. The signal was run through filters and other signal-

processing algorithms. The signal-processing techniques utilized prior knowledge of the expected signals to extract the desired information from the piezoelectric signal. The resultant signal was analyzed through routine techniques, including fast Fourier transform, to identify a primary signal frequency representing respiration and a second signal frequency representing heart rate. However, the signal was acquired with the subject being still and speechless during the data acquisition process.

The difference between the work presented in this work and the work of Sullivan et al. is that Sullivan et al. defined the respiration signal to include only actions relating to respiratory activity. They used signal cancellation to reduce noise in the measured signal. Their work required the patient to hold his or her breath while extracting the heart rate parameters. Moreover, they simply referred to the application of "digital filters and known processing techniques" to achieve the separation of the signals.

In a previous publication [138], Al Ahmad and Al Shareef proposed the use of the piezoelectric sheet as a contactless cardiac cycle sensor to extract heart rate and blood pressure from the measured output voltage. The employed piezoelectric sheet captures the heart mechanical actions. The generated output electrical voltage is conformally mapped with the heart mechanical activity, as has been presented in another work [139]. The measurements performed in both reports do require the patient to hold his or her breath to eliminate the respiration cycle effect.

The current work represents a paradigm shift for estimating the hold-breathing signal from the respiration signal. The experimental outcomes reveal the power of the proposed technique in terms of the high similarity between the measured and constructed signals. This approach will facilitate the development of new sensors to

detect and identify respiration and heart abnormalities. Hence, this algorithm proved its ability to extract heart rate signals utilizing piezoelectric sensors placed away from the heart position, which is beneficial for patients with special conditions.

## 4.8 Summary

This study proposed a novel piezoelectric-based technique to extract the hold-breathing signal from the breathing signal utilizing piezoelectric theory and signal-processing techniques. The piezoelectric-based transducer, which is placed on the subject's chest, is used to collect the breathing signals. The piezoelectric transducer provides noninvasive and contactless connections. With the current approach, the patient is no longer required to hold his or her breath to collect the cardiac signals, as is required by other methods. The study outcomes revealed that the developed technique is simple, reliable, and easy to handle; therefore, it causes minimal inconvenience to clinics and patients, particularly heart patients with special conditions.

## Chapter 5: Conclusion and Future Work

### 5.1 Conclusions

This thesis addresses the development of continuous measurements of multiple vital signs simultaneously utilizing a piezoelectric sensor.

The utilized piezoelectric sensor incorporates a piezoelectric thin film sheet that can be characterized using its corresponding piezoelectric constant, namely $d_{33}$ and $d_{31}$. These constants represents the activity of piezoelectric material. Higher values of $d_{33}$ and $d_{31}$ will produce a higher output voltage signal corresponding to an applied mechanical stress or strain.

When a piezoelectric sheet is placed on the external surface of a human chest, an output voltage that is conformally mapped with the cardiorespiratory activities is produced. Changes and variations of the voltage signal in terms of amplitude and period reflect the respiration rate and heartbeat as well as the blood pressure values. Hence, such values can be extracted from the corresponding voltage signal using the developed algorithms using the piezoelectric sheet and the advancements in signal processing.

It has been found that blood pressure values can be extracted from the output voltage signal provided that the subject holds his or her breath. This thesis contributes to the development of a methodology and algorithm to extract the hold-breathing signal from the measured representative output voltage that corresponds to the respiration and cardiac simultaneous activities. This signal has been identified as the corresponding output voltage signal as a result of the cardiac activities alone,.

Both respiration and heart beats per minutes can be computed in the conventional way by directly counting total number of beats in one minutes. In this thesis the rate is calculated by dividing 60 seconds by the average periods of respiration or cardiac cycles in a specific period. The values of the DP and SP pressure can also be computed using the difference in cardiac signal amplitudes and converted to corresponding pressure values.

This work takes a close look on the use of capacitance-voltage measurements for the extraction of double piezoelectric thin film material deposited on the two faces of a flexible steel sheet. Piezoelectric thin film materials have been deposited using RF sputtering technique. A Gamry References 3000 analyzer was used to collect the capacitance-voltage measurements from both layers. The developed algorithm extracts directly the piezoelectric coefficients knowing the film thickness, the applied voltage, and the capacitance ratio. The capacitance ratio is the ratio between the capacitances of the film when the applied field is antiparallel and parallel to the polling field direction, respectively. The method has been calibrated using a piezoelectric bulk ceramic and validated by comparing the results with the reported values in the literature. The extracted values using the current approach match well the values extracted by other existing methods.

This work further contributes to the extraction of the corresponding representative vital signs directly from the measured respiration signal. The contraction and expansion of the heart muscles, as well as the respiration activities, will induce a mechanical vibration across the chest wall. This vibration can be converted into an electrical output voltage via piezoelectric sensors. During breathing, the measured voltage signal is composed of the cardiac cycle activities modulated

along with the respiratory cycle activity. The proposed technique employs the principles of piezoelectric and signal-processing methods to extract the corresponding signal of cardiac cycle activities from a breathing signal measured in real time. All the results were validated step by step by a conventional apparatus, with good agreement observed.

The piezoelectric transducer provides noninvasive and contactless connections. With the current approach, the patient is no longer required to hold his or her breath to collect the cardiac signals, as is required by other methods. The study outcomes revealed that the developed technique is simple, reliable, and easy to handle; therefore, it causes minimal inconvenience to clinics and patients, particularly heart patients with special conditions.

**5.2 Future Directions**

The developed sensors and non-invasive simultaneous vital sign methods could be incorporated to a novel wearable piezoelectric-based cardiorespiratory monitoring smart system. A functional prototype that we have named "Piezologist", which utilizes a piezoelectric material sheet sensor and incorporates a MetaWearC board equipped with Bluetooth Low Energy (BLE) has been developed as shown in Figure 21. The Piezologist provides the heart rate, respiration rate, blood pressure values, and the corresponding ECG signal cycles obtained and successfully extracted using the developed algorithms of this work.



Figure 21: Initial working prototype that has been tested and validated

The future direction is to enhance the Piezologist functionality and develop further algorithms for the early detection of abnormalities or variations in the cardiac cycle functionality as well as the respiration. This will accelerate the development of next-generation biomedical smart sensors.

For the future work, canceling the effects of movement should be studied. The existing algorithm of extracting vital signs from the breathing signal can eliminate noise caused by small movements, such as eating and talking. For more accuracy, more

enhancement should be achieved to eliminate the effect of big movements such as running. Furthermore, the extracted vital signs from the sensor could be used to determine and identify the emotional status of the patient. More analysis and data collection need to be performed to be able to correlate the vital signs to emotional status.

The continuous monitoring of ECG signals will produce a large amount of data. Handling this data will require high-performance hardware and software, which will lead to huge energy consumption. Thus, to deal with this issue efficiently, by minimizing resources usages and processing time, an innovative alternative solution should be employed. The deployment of our proposed algorithm will lead to a huge reduction in processing power and time. Such a systems feature a small-sized, lightweight, low-cost, reusable, portable, and reliable cardiorespiratory monitoring wearable device. The high quality of our wearable medical sensor makes it convenient for remote health monitoring and disease detection or even prevention. Future work aims to further explore this area in order to identify the best technologies and approaches.

# References

[1]     K. Ho, K. Yamamot, N. Tsuchiya, K. Kuramoto, S. Kobashi, Y. Hata, and H. Nakajima, "Multi Sensor Approach to Detection of Heartbeat and Respiratory Rate Aided by Fuzzy Logic," IEEE, pp. 1-6, 2010.

[2]     M. Hashem, R. Shams, M. Kader, and M. Sayed, "Design and development of a heart rate measuring device using fingertip," in proceedings of International Conference of Computer and Communication Engineering (ICCCE), IEEE, Kuala Lumpur, Malaysia, 2010.

[3]     X. Yang, Z. Chen, S. Chia, H. Lam, S. Ng, J. Teo, and R. Wu, "Textile fiber optic micro bend sensor used for heartbeat and respiration monitoring Sensors," IEEE Sensors, vol. 15, pp. 757-761, 2015.

[4]     M. Carrara, L. Carozzi, S. Cerutti, M. Ferrario, D. Lake, and J. Moorman, "Classification of cardiac rhythm based on heart rate dynamics," in proceedings of 8th Conference of the European Study Group on Cardiovascular Oscillations (ESGCO), IEEE, Trento, Italy, 2014.

[5]     W. Abraham, P. Adamson, M. Packer, J. Bauman, and J. Yadav, "Impact of introduction of pulmonary artery pressure monitoring for heart failure management: longitudinal results from the champion trial," Journal of American Collefge of Cardiology, vol. 63, pp. 1113-1170, 2014.

[6]     D. Mcmanus, J. Riistema, J. Saczynski, F. Kuniyoshi, J. Rock, T. Meyer, N. Teuling, R. Goldberg, and C. Darling, "Transthoracic Bioimpedance Monitoring Predicts Heart Failure Decompensation and Early Readmission after Heart Failure Hospitalization: Preliminary Data from SENTINEL-

HF.," Circulation: Cardiovascular Quality and Outcomes, vol. 319, pp. 1-4, 2014.

[7]     A. Pierre, B. Kreitmann, and G. Habib, "Home Blood Pressure Monitoring in Heart Transplant Recipients: Comparison with Ambulatory Blood Pressure Monitoring," Transplantation, vol. 97, no. 3, pp. 363-367, 2014.

[8]     S. Jansen, S. Spiliopoulos, H. Deng, N. Greatrex, U. Steinseifer, D. Guersoy, R. Koerfer, and G. Tenderich, "A monitoring and physiological control system for determining aortic valve closing with a ventricular assist device," European Journal of Cardiothorac Surgury, vol. 46, no. 3, pp. 356-60, 2014.

[9]     T. Klap and Z. Shina, "Using Piezoelectric Sensor for Continuous-Contact-Free Monitoring of Heart and Respiration Rates in Real-Life Hospital Settings," in Proceedings of CinC, Spain, 22-25 Sept, 2013.

[10]    K. Barrett, S. Barman, S. Boitano, and H. Brooks, "Origin of the Heartbeat & the Electrical Activity of the Heart," in Ganong Phsycology Examination and Board Review, McGraw-Hill Education 25th ed, USA, 2016

[11]    M. Al Ahmad, "Piezoelectric extraction of ECG signal," Scientific Reports, vol. 6, pp. 1-6, 2016.

[12]    X. Xie, Q. Wang, and N. Wu, "A ring piezoelectric energy harvester excited by magnetic forces," International Journal of Engineering Science, vol. 7, pp. 71-78, 2014.

[13]    S. Saadona and O. Sidek, "Micro-Electro-Mechanical System (MEMS)-Based Piezo- electric Energy Harvester for Ambient Vibrations," World Conference on Technol-ogy, Innovation and Entrepreneurship, vol. 195,

pp. 2353-2362, 2015.

[14] K. Moonkeun, H. Beomseok, H. Yong-Hyun, J. Jeong, N. Min, and K. Kwon, "Design, fabrication, and experimental demonstration of a piezoelectric cantilever for a low resonant frequency microelectromechanical system vibration energy harvester," Journal of Micro/NanolithDe-sign, vol. 11, 2012.

[15] X. Xiangdong and W. Quan, "A mathematical model for piezoelectric ring energy harvesting technology from vehicle tires," International Journal of Engineering Science, vol. 94, pp.113-127, 2015.

[16] J. Mei and L. Li, "Double-wall piezoelectric cylindrical energy harvester," Sensors and Actuators, vol. 233, pp. 405-413, 2015.

[17]  A. Dewana, S. Ayb,  M. Karima,  and H. Beyenal, "Alternative power sources for remote, sensors: A review,"  Journal of Power Sources, vol. 245, pp. 129-143, 2014.

[18] K. Wasa, I. Kanno, and H. Kotera, "Fundamentals of thin film piezoelectric materials and processing design for a better energy harvesting MEMS," Power MEMS, vol. 61, pp. 61-66, 2009.

[19] H. Chen, "Power harvesting with PZT ceramics and circuits design," Analog Integration Circuits Signal Process, vol. 62, pp. 263-268, 2010.

[20] Y. Khan, E. miny, C. Ostfeld, M. Lochner, A. Pierre, and A. Arias, "Monitoring of Vital Signs with Flexible and Wearable Medical Devices," Adv Mater, vol. 22, pp. 4373-95, 2016.

[21] C. Chen, D. Hong, A. Wang, and C. Ni, "Fabrication of Flexible Piezoelectric PZT/Fabric Composite," Scientific World Journal, vol. 2013, 2013.

[22]    Y. Chuo, M. Marzencki, B. Hung, C. Jaggernauth, K. Tavakolian, P. Lin, and B. Kaminska, "Mechanically Flexible Wireless Multisensor Platform for Human Physical Activity and Vitals Monitoring," IEEE Transaction on Biomedical Circuits and Systems, vol. 5, pp. 281-94, 2010.

[23]    C. Chen, D. Hong, A. Wang, and C. Ni, "Fabrication of Flexible Piezoelectric PZT/Fabric Composite," Scientific World Journal, vol. 2013, 2013.

[24]    G. Smith, J. Pulskamp, L. Sanchez, D. Potrepka, R. Proie, T. Ivanov, R. Rudy, W. Nothwang, S. Bedair, C. Meyer, and R. Polcawich, "PZT-based piezoelectric MEMS technology," Journal of the American Ceramic Society, vol. 95, no. 6, pp. 1777-1792, 2012.

[25]    C. Sathyanarayana, S. Raja, and H. Ragavendra, "Procedure to Use PZT Sensors in Vibration and Load Measurements," Smart Mat. Res., pp. 1-9, 2013.

[26]    N. Helleputte, M. Konijnenburg, H. Kim, J. Pettine, D. Jee, A. Breeschoten, A. Morgado, T. Torfs, H. Groot, Ch. V. Hoof, and R. Yazicioglu, "A multi-parameter signal-acquisition SoC for connected personal health application," IEEE International Solid-State Circuits Conference, San Francisco, USA, pp. 314-315, 2014.

[27]    N. Davis, "Powering wearables: battery types, current challenges, and energy harvesting," 2015. [online] :
https://www.powerelectronicsnews.com/technology/powering-wearables-battery-types-current-challenges-and-energy-harvesting

[28]    T. Rahman, M. Hasan, A. Farooq, and M. Uddin, "Extraction of cardiac and respiration signals in electrical impedance tomography based on

independent component analysis," Journal of Electronic Bioimpedance, vol. 4, pp. 38-44, 2013.

[29]   A. Vehkaoja, M. Peltokangas, and J. Lekkala, "Extracting the respiration cycle lengths from ECG signal recorded with bed sheet electrodes," Journal of Physics: Conference Series, vol. 459, 2013.

[30]   K. Ho, K. Yamamoto, N. Tsuchiya, K. Kuramoto, S. Kobashi, Y. Hata, and H. Nakajima, "Multi Sensor Approach to Detection of Heartbeat and Respiratory Rate Aided by Fuzzy Logic," IEEE, pp. 1-6, 2010.

[31]   X. Yang, Z. Chen, S. Chia, H. Lam, S. Ng, J. Teo, and R. Wu., "Textile fiber optic micro bend sensor used for heartbeat and respiration monitoring," IEEE Sensors, vol. 15, no. 2, pp. 757-761, 2015.

[32]   I. Smith, J. Mackay, N. Fahrid, and D. Krucheck, "Respiratory rate measurement: a comparison of methods," British Journal of Healthcare Assistants, vol. 05, no. 1, 2011.

[33]   A. Pierre, B. Kreitmann, and G. Habib, "Home Blood Pressure Monitoring in Heart Transplant Recipients: Comparison with Ambulatory Blood Pressure Monitoring," Transplantation, vol. 97, no. 3, pp. 363-367, 2014.

[34]   M. Hashem, R. Shams, M. Kader, and M. Sayed, "Design and development of a heart rate measuring device using fingertip," in proceedings of ICCCE, Malaysia, 2010.

[35]   M. Elliott and A. Coventry "Critical care: the eight vital signs of patient monitoring, British Journal of Nursing," vol. 21, 2012.

[36]   M. Carrara, L. Carozzi, S. Cerutti, M. Ferrario, D. Lake, and J. Moorman, "Classification of cardiac rhythm based on heart rate dynamics," in proceedings of ESGCO, Italy, 2014.

[37]    B. Fernandes, J. Afonso, and R. Simoes, "Vital signs monitoring and management using mobile devices," in proceedings of CISTI, Iberian, July, 2011.

[38]    R. A. Daou, E. Aad, F. Nakhle, A. Hayek, and J. Börcsök, "Patient vital signs monitoring via android application," in proceedings of ICABME, 2015.

[39]    M. Meccariello, D. Perkins, L. Quigley, A. Rock, and J. Qiu, "Evaluating the Use of an Automated Vital Signs Documentation System on a Medical/Surgical Unit," vol. 24, 2010.

[40]    T. Gao, L. Hauenstein, A. Alm, D. Crawford, C. Sims, A. Husain, and D. White, "Vital Signs Monitoring and Patient Tracking Over a Wireless Network," Johns Hopkins APL Technical Digest, vol. 1, pp. 102-105, 2005.

[41]    W. Abraham, P. Adamson, M. Packer, J. Bauman, and J. Yadav, "Impact of introduction of pulmonary artery pressure monitoring for heart failure management: longitudinal results from the champion trial," Presented at ACC.14, 2014.

[42]    D. Mcmanus, J. Riistema, J. Saczynski, F. Kuniyoshi, J. Rock, T. Meyer, N. Teuling, R. Goldberg, and C. Darling, "Transthoracic Bioimpedance Monitoring Predicts Heart Failure Decompensation and Early Readmission after Heart Failure Hospitalization: Preliminary Data from SENTINEL-HF," Circulation: Cardiovascular Quality and Outcomes, vol. 319, pp. 1-4, 2014.

[43]    S. Jansen, S. Spiliopoulos, H. Deng, N. Greatrex, U. Steinseifer, D. Guersoy, R. Koerfer, and G. Tenderich, "A monitoring and physiological

control system for determining aortic valve closing with a ventricular assist device," European Journal of Cardiothorac Surgury, vol. 46, no. 3, pp. 356-60, 2014.

[44]    T. Hall, Y. Donald, C. Lie, T. Nguyen, J. Mayeda, P. Lie, J. Lopez and R. Banister, "Non-Contact Sensor for Long-Term Continuous Vital Signs Monitoring: A Review on Intelligent Phased-Array Doppler Sensor Design," Sensors (Basel), vol. 17, 2017.

[45]    T. Yilmaz, R. Foster, and Y. Hao, "Detecting Vital Signs with Wearable Wireless Sensors," Sensors (Basel), vol. 10, pp. 10837-10862, 2010.

[46]    V. Henrich, "The surfaces of metal oxides," Reports Progress Physics, vol. 48, pp. 1481-1541, 1999.

[47]    M. Sunar, "Recent Advances in Sensing and Control of Flexible Structures Via Piezoelectric Materials Technology," Applied Mechanics, vol. 52, pp. 1-16, 2009.

[48]    C. Sathyanarayana, S. Raja, and H. Ragavendra, "Procedure to Use PZT Sensors in Vibration and Load Measurements," Smart Material Research, pp. 1-9, 2013.

[49]    N. V. Helleputte, M. Konijnenburg, H. Kim, J. Pettine, D-W. Jee, A. Breeschoten, A. Morgado, T. Torfs, H. Groot, C. Hoof, and R. Yazicioglu, "A multi-parameter signal-acquisition SoC for connected personal health applications," in proceedings IEEE Int. Solid-State Circuits Conference, pp. 314-315, 2014.

[50]    K. Wasa, I. Kanno, and H. Kotera, "Fundamentals of thin film piezoelectric materials and processing design for a better energy harvesting MEMS," Power MEMS, vol. 61, pp. 61-66, 2009.

[51]    H. Chen, "Power harvesting with PZT ceramics and circuits design," Analog Integration Circuits Signal Process, vol. 62, pp. 263-268, 2010.

[52]    A. Anis, N. Nordin, R. Othman, and H. Salleh, "Design, simulation and fabrication of piezoelectric micro generators for aero acoustic applications," Microsystems Technology, vol. 17, pp. 563-573, 2011.

[53]    Y. Khan, M. Ostfeld, C. Lochner, A. Pierre, and A. Arias, "Monitoring of Vital Signs with Flexible and Wearable Medical Devices," Advanced Material, vol. 22, pp. 4373-95, 2016.

[54]    C. Chen, D. Hong, A. Wang, and C. Ni, "Fabrication of Flexible Piezoelectric PZT/Fabric Composite," The Scientific World Journal, vol. 2013, pp. 1-4, 2013.

[55]    Y. Chuo, M. Marzencki, B. Hung, C. Jaggernauth, K. Tavakolian, P. Lin, and B. Kaminska, "Mechanically Flexible Wireless Multisensor Platform for Human Physical Activity and Vitals Monitoring," IEEE Transaction on Biomedical Circuits and Systems, vol. 5, pp. 281-94, 2010.

[56]    H-J. Tseng, V-C. Tian, and W-J. Wu, "Flexible PZT Thin Film Tactile Sensor for Biomedical Monitoring," Sensors, vol. 13, pp. 5478-5492, 2013.

[57]    J. Son, G-T. Hwang, C. Jeong, J. Ryu, M. Koo, I. Choi, S. Lee, M. Byun, Z. Wang, and K. Lee, "Highly-Efficient, Flexible Piezoelectric PZT Thin Film Nanogenerator on Plastic Substrates," Advanced Materials, vol. 26, no. 16, pp. 2514-2520, 2014.

[58]    G-T. Hwang, M. Byun, C. Jeong, and K. Lee, "Flexible Piezoelectric Thin-Film Energy Harvesters and Nanosensors for Biomedical Applications," Advanced Material, vol. 4, pp. 646-658, 2015.

[59]    B. XU, S. Buhler, K. Litiau, S. Elrod, S. Uckun, V. Hafiychuk, and V. Smelyanskiy, "Novel Approach to Make Low Cost, High Density PZT Phased Array and Its Application in Structural Health Monitoring," International Workshop on Strength Health Monitoring, 2009.

[60]    V. Uskoković, "The role of hydroxyl channel in defining selected physicochemical peculiarities exhibited by hydroxyapatite," PMC, vol. 5, pp. 6614-36633, 2015.

[61]    N. Jackson, O. Olszewski, L. Keeney, A. Blake, and A. Mathewson, "A Capacitive based Piezoelectric AlN Film Quality Test Structure," Microelectronic Test Structures (ICMTS), International Conference, USA, 2015.

[62]    H. Tabatabai, D. Oliver, J. Rohrbaugh, and C. Papadopoulo, "Novel Applications of Laser Doppler Vibration Measurements to Medical Imaging," Sensing and Imaging: An International Journal, vol. 14, pp. 1413-28, 2013.

[63]    D. Berlincourt and H. Jaffe, "Elastic and piezoelectric coefficients of single-crystal barıμm titanate," Physics Review, vol. 111, pp. 143, 1958.

[64]    K. Tonisch, V. Cimalla, C. Foerster, D. Dontsov, and O. Ambacher, "Piezoelectric properties of thin AlN layers for MEMS application determined by piezoresponse force microscopy," Physics Status Solidi, vol. 3, pp. 2274-2277, 2006.

[65]    N. Jackson, O. Olszewski, L. Keeney, A. Blake, and A. Mathewson, "A capacitive based piezoelectric AlN film quality test structure," International Conference on Microelectronic Test Structures (ICMTS), USA, pp. 193-197, 2015.

[66] T. Hemert, D. Sarakiotis, S. Jose, R. Hueting, and J. Schmitz, "Exploring capacitance-voltage measurements to find the piezoelectric coefficient of aluminum nitride," in proceeding of Micro Test Structure (ICMTS), 2011 IEEE Int. Con. Netherlands, 2011.

[67] T. Hemert, K. Reimann, and R. Hueting, "Extraction of second order piezoelectric parameters in bulk acoustic wave resonators, Applied physics Letters, vol. 100, 2012.

[68] M. Zhang , J. Yang, C. Si, G. Han, Y. Zhao, and J. Ning, "Research on the piezoelectric properties of AlN thin films for MEMS applications," Micromachines, vol. 6, pp. 1236-1248, 2015.

[69] X. Yang, Z. Chen, S. Chia, H. Lam, S. Ng, J. Teo, and R. Wu, "Textile fiber optic micro bend sensor used for heartbeat and respiration monitoring," Sens. IEEE Sensors, vol. 15, pp. 757-761, 2015.

[70] I. Smith, J. Mackay, N. Fahrid, and D. Krucheck, "Respiratory rate measurement: a comparison of methods," British Journal of Healthcare Assistants, vol. 05, no. 01, 2011.

[71] A. Pierre, B. Kreitmann, and G. Habib, "Home Blood Pressure Monitoring in Heart Transplant Recipients: Comparison with Ambulatory Blood Pressure Monitoring," Transplantation, vol. 97, no.3, pp. 363-367, 2014.

[72] M. Hashem, R. Shams, M. Kader, and M. Sayed, "Design and development of a heart rate measuring device using fingertip," in proceedings of ICCCE, Malaysia, 2010.

[73] K. Ho, K. Yamamoto, N. Tsuchiya, K. Kuramoto, S. Kobas, Y. Hata, and H. Nakajima, "Multi Sensor Approach to Detection of Heartbeat and Respiratory Rate Aided by Fuzzy Logic," IEEE, pp. 1-6, 2010.

[74] M. Elliott and A. Coventry, "Critical care: the eight vital signs of patient monitoring, British Journal of Nursing," vol. 21, no. 10, 2012.

[75] M. Carrara, L. Carozzi, S. Cerutti, M. Ferrario, D. Lake, and J. Moorman, "Classification of cardiac rhythm based on heart rate dynamics," in ESGCO, Italy, 2014.

[76] B. Fernandes, J. Afonso, and R. Simoes, "Vital signs monitoring and management using mobile devices," in proceedings of CISTI, Iberian, July 2011.

[77] R. Daou, E. Aad, F. Nakhle, A. Hayek, and J. Börcsök, "Patient vital signs monitoring via android application," in proceedings of ICABME, 2015.

[78] M. Cardona-Morrell, M. Prgomet , R. Lake , M. Nicholson, R. Harrison, J. Long, J. Westbrook, J. Braithwaite, and K Hillman, "Vital signs monitoring and nurse–patient interaction: A qualitative observational study of hospital practice, International Journal of Nursing Studies," vol. 56, pp. 9-16, 2016.

[79] M. Meccariello, D. Perkins; L. Quigley, A. Rock, and J. Qiu, "Evaluating the Use of an Automated Vital Signs Documentation System on a Medical/Surgical Unit," vol. 24, 2010.

[80] T. Gao, L. Hauenstein, A. Alm, D. Crawford, C. Sims, A. Husain, and D. White, "Vital Signs Monitoring and Patient Tracking Over a Wireless Network," Johns Hopkins APL Technical Digest, vol. 27, 2006.

[81] W. Abraham, P. Adamson, M. Packer, J. Bauman, and J. Yadav, "Impact of introduction of pulmonary artery pressure monitoring for heart failure

management: longitudinal results from the champion trial," Presented at ACC.14, 2014.

[82] D. Mcmanus, J. Riistema, J. Saczynski, F. Kuniyoshi, J. Rock, T. Meyer, N. Teuling, R. Goldberg, and C. Darling, "Transthoracic Bioimpedance Monitoring Predicts Heart Failure Decompensation and Early Readmission after Heart Failure Hospitalization: Preliminary Data from SENTINEL-HF," Circulation: Cardiovascular Quality and Outcomes, vol. 319, pp. 1-4, 2014.

[83] S. Jansen, S. Spiliopoulos, H. Deng, N. Greatrex, U. Steinseifer, D. Guersoy, R. Koerfer, and G. Tenderich, "A monitoring and physiological control system for determining aortic valve closing with a ventricular assist device," European Journal of Cardiothorac Surgery, vol. 46, no. 3, pp. 356-60, 2014.

[84] T. Hall, Y. Donald, C. Lie, T. Nguyen, J. C. Mayeda, P. Lie, J. Lopez and R. Banister, "Non-Contact Sensor for Long-Term Continuous Vital Signs Monitoring: A Review on Intelligent Phased-Array Doppler Sensor Design," Sensors (Basel), vol. 17, no. 11, 2017.

[85] T. Yilmaz, R. Foster, and Y. Hao, "Detecting Vital Signs with Wearable Wireless Sensors," Sensors (Basel), vol. 10, no. 12, pp. 10837-10862, 2010.

[86] M. Jessica, J. Kelly, R. trecker, and M. Bianchi, "Recent Developments in Home Sleep-Monitoring Devices," ISRN neurology, 2012.

[87] I. Landsman, S. Hays, C. Karsanac, and A. Franklin, "Chapter 13 – Pediatric Anesthesia," in Pediatric Surgery, 7th ed, pp. 201-226 2012.

[88]     T. Seres, and A. Secrets, "CHAPTER 68 – Heart Transplantation," 4th ed., pp. 473-479, 2011.

[89]     S. Rampersad, K. Schenkman, and L. Martin, "Chapter 43 – Noninvasive Monitoring in Children," in Pediatric Critical Care, 4th ed., pp. 550-560, 2011.

[90]     L. Ren, H. Wang, K. Naishadham , Q. Liu, and A. Fath, "Non-Invasive Detection of Cardiac and Respiratory Rates from Stepped Frequency Continuous Wave Radar Measurements Using the State Space Method," in proceedings of Symposium, Phoenix, AZ, USA, 2015.

[91]     J. Patterson, D. Mcilwraith, and G. Yang, "A flexible, low noise reflective PPG sensor platform for ear-worn heart rate monitoring," in Proceedings of the Sixth International Workshop on Wearable and Implantable Body Sensor Networks, USA, Washington DC, pp. 286-291, 3-5 June 2009.

[92]     J. Lee, J. Heo, W. Lee, Y. Lim, Y. Kim, and K. Park, "Flexible capacitive electrodes for minimizing motion artifacts in ambulatory electrocardiograms," Sensors, vol. 14, pp. 14732-14743, 2014.

[93]     W. Abraham, P. Adamson, M. Packer, J. Bauman, and J. Yadav, "Impact of introduction of pulmonary artery pressure monitoring for heart failure management: longitudinal results from the champion trial," Journal of the American College of Cardiology, vol. 63, pp. 1113-1170, 2014.

[94]     D. Mcmanus, J. Riistema, J. Saczynski, F. Kuniyoshi, J. Rock, T. Meyer, N. Teuling, R. Goldberg, and C. Darling, "Transthoracic Bioimpedance Monitoring Predicts Heart Failure Decompensation and Early Readmission after Heart Failure Hospitalization: Preliminary Data from SENTINEL-

HF," Circulation: Cardiovascular Quality and Outcomes, vol. 319, pp. 1-4, 2014.

[95]    J. Patterson, D. McIlwraith, and G. Yang, "A flexible, low noise reflective PPG sensor platform for ear-worn heart rate monitoring," in proceedings of the Sixth International Workshop on Wearable and Implantable Body Sensor Networks, Washington DC, USA, pp. 286-291, 2009.

[96]    J. Lee, J. Heo, W. Lee, Y. Lim, Y. Kim, and K. Park, "Flexible capacitive electrodes for minimizing motion artifacts in ambulatory electrocardiograms," Sensors, vol. 14, pp. 14732-14743, 2014.

[97]    J. Shin, S. Hwang, M. Chang, and K. Park, "Heart rate variability analysis using a ballistocardiogram during Valsalva manoeuvre and post exercise," Physiological Measurement, vol. 32, no. 8, pp. 1239-1264, 2011.

[98]    J. Kortelainen and J. Pärkkä, "Multichannel bed pressure sensor for sleep monitoring," in proceedings of Computing in Cardiology, Poland, 9-12 Sept, 2012.

[99]    E. Pinheiro, O. Postolache, and P. Girão, "Blood Pressure and Heart Rate Variabilities Estimation Using Ballistocardiography," in proceedings of Telecommunications - ConfTele, Santa Maria da Feira, Portugal, vol. 1, pp. 125-128, May, 2009.

[100]  T. Rahman, M. Hasan, A. Farooq, and M. Uddin, "Extraction of cardiac and respiration signals in electrical impedance tomography based on independent component analysis," Journal of Electronics Bioimpedence, vol. 4, pp. 38-44, 2013.

[101]  J. Deibele, H. Luepschen, and S. Leonhardt, "Dynamic separation of pulmonary and cardiac changes in electrical impedance tomography," Physiological Measurements, vol. 29, pp. S1-14, 2008.

[102]  O. Inan, M. Pouyan, A. Javaid, S. Dowling, M. Etemadi, A. Dorier, and L. Klein, "Novel Wearable Seismocardiography and Machine Learning Algorithms Can Assess Clinical Status of Heart Failure Patients," Circulation: Heart Failure, vol. 11, 2018.

[103]  A. Vehkaoja, M. Peltokangas, and J. Lekkala, "Extracting the respiration cycle lengths from ECG signal recorded with bed sheet electrodes," Journal of Physics: Conference Series, vol. 459, 2013.

[104]  P. Bifulco, G. Gargiulo, G. d'Angelo, A. Liccardo, M. Romano, F. Clemente, and M. Cesarelli, "Monitoring of respiration, seismocardiogram and heart sounds by a PVDF piezo film sensor," 20th IMEKO TC4, 2014.

[105]  T. Klap and Z. Shina, "Using Piezoelectric Sensor for Continuous-Contact-Free Monitoring of Heart and Respiration Rates in Real-Life Hospital Settings," in proceedings of CinC, Spain, pp. 22-25, 2013.

[106]  S. Yoon and Y. Cho, "A Skin-attachable Flexible Piezoelectric Pulse Wave Energy Harvester," Journal of Physics Conference Series, vol. 557, pp. 1-5, 2014.

[107]  S. Yoon and Y. Cho, "A Skin-attachable Flexible Piezoelectric Pulse Wave Energy Harvester," Journal of Physics Conference Series, vol. 557, pp. 1-5, 2014.

[108]  Y. Chang, J. Lee, and K. Kim, "Heartbeat Monitoring Technique Based on Corona-Polled PVDF Film Sensor for Smart Appare l Application," Solid State Phenom, pp. 299-302, 2007.

[109] D. Buxi, J. Penders, and C. van Hoof, "Early results on wrist based heart rate monitoring using mechanical transducers," in proceedings of the Annual International Conference of the IEEE Engineering in Medicine and Biology Society, Buenos Aires, Argentina, pp. 4407-4410, 2010.

[110] G. Guerrero, J. Kortelainen, E. Palacios, A. Bianchi, G. Tachino, M. Tenhunen, and M. Gils, "Detection of sleep-disordered breathing with Pressure Bed Sensor," 35th Annual International Conference of the IEEE Engineering in Medicine and Biology Society (EMBC), 2013.

[111] A. Tal, Z. Shinar, D. Shaki, S. Codish, and A. Goldbart, "Validation of Contact-Free Sleep Monitoring Device with Comparison to Polysomnography," Journal of clinical sleep medicine, vol. 15, no. 3, pp. 517-522, 2017.

[112] Sh. Sato, T. Koyama, K. Ono, G. Igarashi, H. Watanabe, H. Ito, and M. Muraoka, "Cardiac Diagnosing by a Piezoelectric-transducer-based Heart Sound Monitor System," in proceedings of the International Conference on Biomedical Electronics and Devices, Rome, Italy, 26-29 January, 2011.

[113] P. Bifulco, G. Gargiulo, G. d'Angelo, A. Liccardo, M. Romano, F. Clemente, and M. Cesarelli, "Monitoring of respiration, seismocardiogram and heart sounds by a PVDF piezo film sensor," in proceedings of 20th IMEKO TC4, Benevento, Italy, 2014.

[114] T. Klap and Z. Shina, "Using Piezoelectric Sensor for Continuous-Contact-Free Monitoring of Heart and Respiration Rates in Real-Life Hospital Settings," in proceedings of CinC, Spain, 22-25 Sept. 2013.

[115] N. Mizuno and N. ManhHiep, "An Adaptive Filtering Technique for Driver's Heart Rate Monitoring through Vibration Signal by Seat-

Embedded Piezoelectric Sensors," in proceedings of IFAC, vol. 46, no. 11, pp. 647-652, 2013.

[116]   M. Al Ahmad, "Piezoelectric extraction of ECG signal," Scientific Reports, vol. 6, pp. 1-6, 2016.

[117]   K. Barrett, S. Barman, S. Boitano, and H. Brooks, "Origin of the Heartbeat & the Electrical Activity of the Heart," in Ganong Phsycology Examination and Board Review, McGraw-Hill Education 25th ed, USA, 2016.

[118]   K. Nakasho,  H. Madokoro,  and N. Shimoi, "Implementation of a vital signs monitoring system in combination with a bed-leaving detection system," System Integration (SII), IEEE/SICE International Symposium on, 2016.

[119]   N. Al Taradeh, N. Bastaki, I. Saadat, and M. Al Ahmad, "Non-invasive piezoelectric detection of heartbeat rate and blood pressure," Electronics Letters, vol. 51, pp. 452-454, 2015.

[120]   United Arab Emirates Ministry of Health and Prevention website [Online]: http://www.mohap.gov.ae/en/AwarenessCenter/Pages/health-statistics.aspx

[121]   A. Khaligh, P. Chapman, and R. Ghodssi, "Guest Editorial," IEEE Trans. on Industrial Electronics, vol. 57, no. 3, pp. 810-812, 2010.

[122]   J. Rocha, L. Goncalves, P. Rocha, M. Silva, and S. Lanceros-Mendez, "Energy Harvesting From Piezoelectric Materials Fully Integrated in Footwear," IEEE Trans. on Industrial Electronics, vol. 57, no. 3, pp. 813-819 , 2010.

[123]   S. Mehraeen, S. Jagannathan, and K. Corzine, "Energy Harvesting From Vibration With Alternate Scavenging Circuitry and Tapered Cantilever

Beam," IEEE Trans. on Industrial Electronics, vol. 57, no. 3, pp. 820-830, 2010.

[124] C. Liu, K. Chau, and X. Zhang, "An Efficient Wind–Photovoltaic Hybrid Generation System Using Doubly Excited Permanent-Magnet Brushless Machine," IEEE Trans. on Industrial Electronics, vol. 57, no. 3, pp. 831-839, 2010.

[125] A. Tabesh and L. Frechette, "A Low-Power Stand-Alone Adaptive Circuit for Harvesting Energy from a Piezoelectric Micropower Generator," IEEE Trans. on Industrial Electronics, vol. 57, no. 3, pp. 840-849, March 2010.

[126] A. Khaligh, P. Zeng, and C. Zheng, "Kinetic Energy Harvesting Using Piezoelectric and Electromagnetic Technologies—State of the Art," IEEE Trans. on Industrial Electronics, vol. 57, no. 3, pp. 850-860, 2010.

[127] J. Carmo, L. Goncalves, and J. Correia, "Thermoelectric Microconverter for Energy Harvesting Systems," IEEE Trans. on Industrial Electronics, vol. 57, no. 3, pp. 861-867, 2010.

[128] W. Li, S. He, and Sh. Yu, "Improving Power Density of a Cantilever Piezoelectric Power Harvester Through a Curved L-Shaped Proof Mass," IEEE Trans. on Industrial Electronics, vol. 57, no. 3, pp. 868-876, 2010.

[129] A. Miraoui, J. Kolar, and M. Pucci, "Guest Editorial," IEEE Transaction on Industrial Electronics, vol. 57, no. 3, pp. 877-880, 2010.

[130] R. Torah, S. Beeby, and N. White, "Experimental investigation into the effect of substrate clamping on the piezoelectric behavior of thick-film PZT elements," Journal of Physics D: Applied Physics, vol. 37, pp. 1074-1078, 2004.

[131] Piezoelectric Ceramics: Principles and Applications, APC International Ltd., APC International Ltd, 2002.

[132] J. Shepard, P. Moses, and S. Trolier-McKinstry, "The Wafer Flexure Technique for the Determination of the Transverse Piezoelectric Coefficient (d31) of PZT Thin Films," Sensors and Actuator, vol. 71, pp. 133-138, 1998.

[133] D. Royer and V. Kmetik, "Measurement of piezoelectric constants using an optical heterodyne interferometer", Electronic Letters, vol. 28, no. 19, pp. 1828-1830, 1992.

[134] P. Muralt, "Ferroelectric thin films for micro-sensor and actuators," Journal of Micromechanics Microengineering, vol. 10, pp. 136-146, 2000.

[135] G. Farnell, I. Cermak, P. Silvester and S. Wong, "Capacitance and field distributions for interdigital surface-wave transducers", IEEE Trans. Sonics Ultrasonics, vol. SU-17, pp. 188-195, 1970.

[136] D. Berlincourt and H. Jaffe, "Elastic and piezoelectric coefficients of single-crystal barium titanate," Physics Review, vol. 111, no. 1, pp. 143–148, 1958.

[137] P. Sanz-González, J. Hernando, J. Vazquez, and J. Sanchez-Rojas, "Resonance frequencies and modal shape characterization of piezoelectric microcantilevers," in proceedings of SPIE 6589, Smart Sensors, Actuators, and MEMS III, vol. 65890L, 2007.

[138] M. Al Ahmad and H. Al Shareef, "A Capacitance-Based Methodology for the Estimation of Piezoelectric Coefficients of Polled Piezoelectric Materials," Electrochemical Solid-State Letters, vol. 13, no. 12, pp. 108-110, 2010.

[139]   M. Al Ahmad and R. Plana, "Piezoelectric Coefficients of Thin Film Aluminum Nitride Characterizations Using Capacitance Measurements," IEEE Microwave and Wireless Components Letters, vol. 19, no. 3, pp. 140-142, 2009.

[140]   A. Ledoux, "Theory of piezoelectric materials and their applications in civil engineering," Ms.c. thesis, Department of Civil Engineering, MIT, MA, USA, 2011.

[141]   S. Roundy and P. Wright, "A piezoelectric vibration based generator for wireless electronics," Smart Material Structures, vol. 13, no. 5, pp. 1131-1142, 2004.

[142]   M. Al Ahmad, "Piezoelectric extraction of ECG signal," Scientific Reports, vol. 6, pp. 1-6, 2016.

[143]   M. Al Ahmad, A. El shurafa, K. Salama, and H. Al shareef, "Determination of maximum power transfer conditions of bimorph piezoelectric energy harvesters," Journal of Applied Physics, vol. 111, no. 10, 2012.

[144]   Datasheet [Online]: https://matthey.com//media/files/products/technical-data-sheets/piezo-medical-components-tds.pdf.

[145]   S. Stach, D. Dallaeva, S. Talu, P. Kaspar, P. Tomanek, S. Giovanzana, and L. Gramela, "Morphological features in aluminum nitride epilayers prepared by magnetron sputtering," Material Science, vol. 33, pp. 175-184, 2015.

[146]   M. Wei, "Development of Electroplated-Ni Structured Micromechanical Resonators for RF Application," Ph.D. dissertation, Department of Electrical Engineering, University Of South Florida, FA, USA, 2014.

[147] M. Al Ahmad and H. N. Al shareef, "A Capacitance-Based Methodology for the Estimation of Piezoelectric Coefficients of Polled Piezoelectric Materials," Electrochemical and Solid-State Letters, vol. 13, no. 12, pp. G108-G110, 2010.

[148] K. Suu, "Advanced in Ferroelectronics," in Advanced in Ferroelectronics, 2012.

[149] K. Barrett, S. Barman, S. Boitano, and H. Brooks , "Origin of the Heartbeat & the Electrical Activity of the Heart," in Ganong Phsycology Examination and Board Review, McGraw-Hill Education 25th ed, USA, 2016.

[150] K. Nakasho, H. Madokoro, and N. Shimoi, "Implementation of a vital signs monitoring system in combination with a bed-leaving detection system," in proceedings of System Integration (SII), IEEE/SICE International Symposium on, 2016.

[151] N. Al Taradeh, N. Bastaki, I. Saadat, and M. Al Ahmad, "Non-invasive piezoelectric detection of heartbeat rate and blood pressure," Electronics Letters, vol. 51, pp. 452-454, 2015.

[152] P. Chiale, D. Etcheverry, J. Pastori, P. Fernandez, H. Garro, M. González, and M. Elizari, "The multiple electrocardiographic manifestations of ventricular repolarization memory," Current Cardiology Reviews, vol. 10, no. 3, pp. 190-201, 2014.

[153] L. Alton, B. Gulli, and, J. Krohmer "The Human Body," Thygerson, in First Aid CPR and AED, 5th ed, USA,Jones & Bartlett Learning, pp. 31-32, 2017.

[154]  G. Thibodeau and K. Patton, "Organ Systems of the Body," in Structure and Function of the Body, Mosby Year Book, 11th ed, USA,  pp. 71-83, 1997.

[155]  G. Doetsch, "Applications of the Convolution Theorem: Integral Relations," In: Introduction to the Theory and Application of the Laplace Transformation, Springer-Verlag, Berlin Heidelberg, 1974.

[156]  R. Bracewell, "The Fourier Transform and Its Applications," 3rd ed., McGraw-Hill Science/Engineering/Math, June 8, 1999.

[157]  P. Sullivan, K. Cheung, C. Sullivan, and P. Pernambuco-Wise, "Passive physiological monitoring (p2m) system," US 2012/0259179 A1, 11/2012.

[158]  Ü. Sağlam, "Analyzing the Efficiencies of Renewable Energy Sources with Data Envelopment Analysis," in proceedings of 2016 Annual Meeting of the Decision Sciences Institute, Austin, Texas, 2016.

[159]  S. Weart, "The Discovery of the Risk of Global Warming," Physics Today, vol. 50, pp. 1-34, 1997.

[160]  S. Krantz, "Principles of Fourier Analysis," Charman & HALL/CRC Kenneth B. Howell Department of Mathematical Science University of Alabama in Huntsville Principles of Fourier Analysis Boca Raton London New York Washington, D.C, 2001.

[161]  J. Smith, "Mathematica of the discrete fourier transform with audio applications," Center for Computer Research in Music and Acoustics (CCRMA) , Department of Music, Stanford University, Stanford, California 94305 USA, 2002.

[162]  C. Blackwell and R. Simpson, "The Convolution Theorem in Modern Analysis," transactions of education, 1966.

[163]  G. A. Cervantes, "Technical Fundamentals of Radiology," chapter 16, Mathematical analysis of convolution, May 2016 .

[164]  D. Champeney, "A Handbook of Fourier Theorems," Cambridge University Press, 1987.

[165]  I. Hirschman, editor: D. Widder "The Convolution Transform," (Dover Books on Mathematics) Paperback, March 11, 2005.

## List of Publications

- Areen Allataifeh and Mahmoud Al Ahmad, "Comparison between piezoelectric plate and hollow cylinder-based energy harvesters", IEEE WIECON-ECE, pp. 98 – 101, Bangladesh, 2015.

- Mahmoud Al Ahmad, and Areen Allataifeh, "Piezoelectric-based Energy Harvesting for Smart City Application", in Information Innovation Technology in Smart Cities, Springer, Dubai, UAE, 2016.

- Areen Allataifeh, Mahmoud Al Ahmad, "Synthesizing Equivalent Electric Circuit for Respiration and Cardiac Signals", ICETAS 2107, Bahrain.

- Areen Allataifeh, Mahmoud Al Ahmad, "Highly Sensitive Piezo-Based Touch Sensor for Robotics Applications," ISMA18, Sharjah, 2017.

- Mahmoud Al Ahmad and Areen Allataifeh, "Electrical extraction of piezoelectric constants", Journal of HELIYON, Elsevier, vol. 4, pp. 1-15, 2018.

**Patent**

"Self-Biased Sensing Device Methods of Fabricating and Operating Same", Mahmoud Al Ahmad, Areen Allataifeh, US20180195921A1, 2016.

# Appendix

## A. Fourier transform

The French mathematician, Fourier born in 1768 in France [158], came up with this transform along with Jean Baptiste Joseph in his thirties while trying to solve some agriculture problems. He wanted to understand heat flow in the ground due to the fact that the ground constant temperature deep down whereas on the surface it is cold at night and hot during the day [159].

The Fourier transform is considered to be a mathematical technique that converts functions from time domain to frequency domain [160]. It can be defined for infinite continuous time and frequency domain signals. The forward Fourier transform can be defined as follows:

$$F(k) = \int_{-\infty}^{\infty} f(x)e^{-2\pi ikx}dk \tag{32}$$

where $F(k)$ is a complex-valued function of $k$, its domain is a set of real numbers $k$ and defined on the frequency domain while the original signal $f(x)$ defined on the time domain. The inverse Fourier transform is defined as follows:

$$f(k) = \int_{-\infty}^{\infty} F(x)e^{2\pi ikx}dk \tag{33}$$

The Fourier transform maps the time series into a series of frequencies with phases and amplitudes that form the time series, while the inverse Fourier transform in return conforms back the corresponding time series from the series of frequencies. It is worth noting that $F(k)$ is a complex-valued, transformed function that is equivalent to $f(x)$ but has completely different properties [161].

## B. Convolution theory

In electrical engineering applications, there is a need to deal with multiplication in the time domain and find the result in the frequency domain. Therefore, the convolution theorem is significant [162].

The convolution theorem implies that if the Fourier transform of a convolution is taken, it represents the point-wise product of Fourier transforms at particular conditions. Simply, the convolution in the time domain is equivalent to the point-wise product of the frequency domain functions [163].

The central limit theorem is one of the deductions of the convolution theorem. It is significant in probability theory as it illustrates the reason Gaussian probability distribution is observed in nature. The central limit theorem implies that when the variable is the sum of finite variance and mean random processes, then the Gaussian distribution results. The sum of the processes have a Gaussian distribution even if each component does not [164].

There are various applications of the convolution such as digital image processing, for which is used in edge detection, the echo is the sound convolution in linear acoustics, artificial reverberation as the convolution is used to map the room impulse response on digital video in physics for solving the superposition problems; and in statistics, computational fluid dynamics, probability theory, and optics [120]. The expressions of the convolution theorem are as follows [165]:

$$w(t) = u(t)v(t) \quad \leftrightarrow \quad W(f) = U(f) * V(f) \tag{34}$$

$$w(t) = u(t) * v(t) \quad \leftrightarrow \quad W(f) = U(f)V(f) \tag{35}$$

It could be noted that the convolution theorem is commutative:

$$u(t) * v(t) = v(t) * u(t) \tag{36}$$

Associative:

$$u(t) * v(t) * w(t) = \big(u(t) * v(t)\big) * w(t) = u(t) * (v(t) * w(t)) \tag{37}$$

And could be also distributed over addition operation:

$$w(t) * \big(u(t) + v(t)\big) = w(t) * u(t) + w(t) * v(t) \tag{38}$$

## C. Sensor placement

In order to get the respiration signal, the sensor is placed on the chest at the left side. A double sided adhesive medical tape was used to attach the sensor on the chest as shown in Figure 22.



Figure 22: Double sided adhesive medical tape

The tape was shaped as circles to take the shape of the bottom side of the sensor, then one side of the tape is attached to the sensor.